NATIONAL ADVISORY COMMITTEE FOR AERONAUTICS

TECHNICAL MEMORANDUM

No. 1183

TEMPERATURES AND STRESSES ON HOLLOW BLADES FOR GAS TURBINES

By Erich Pollmann

TRANSLATION

"Temperaturen und Beanspruchungen an Hohlschaufeln für Gasturbinen"
Deutsche Luftfahrtforschung, Forschungsbericht Nr. 1879

Washington
September 1947

NATIONAL ADVISORY COMMITTEE FOR AERONAUTICS

TECHNICAL MEMORANDUM NO. 1183

TEMPERATURES AND STRESSES ON HOLLOW BLADES FOR GAS TURBINES*

By Erich Pollmann

Abstract: The present treatise reports on theoretical investigations and test-stand measurements which were carried out in the BMW Flugmotoren GmbH in developing the hollow blade for exhaust gas turbines. As an introduction the temperature variation and the stress on a turbine blade for a gas temperature of 900° and circumferential velocities of 300 meters per second are discussed. The assumptions on the heat transfer coefficients at the blade profile are supported by tests on an electrically heated blade model. The temperature distribution in the cross section of a blade is thoroughly investigated and the temperature field determined for a special case. A method for calculation of the thermal stresses in turbine blades for a given temperature distribution is indicated. The effect of the heat radiation on the blade temperature also is dealt with. Test-stand experiments on turbine blades are evaluated, particularly with respect to temperature distribution in the cross section; maximum and minimum temperature in the cross section are ascertained. Finally, the application of the hollow blade for a stationary gas turbine is investigated. Starting from a setup for 550° C gas temperature the improvement of the thermal efficiency and the fuel consumption are considered as well as the increase of the useful power by use of high temperatures. The power required for blade cooling is taken into account. The possibility to apply high circumferential velocities with good efficiency is discussed.

Outline: I. Introduction

II. Temperature variation and stress along the blade with heat conduction to the rotor disc

*"Temperaturen und Beanspruchungen an Hohlschaufeln für Gasturbinen." Zentrale für wissenschaftliches Berichtswesen der Luftfahrtforschung des Generalluftzeugmeisters (ZWB) Berlin-Adlershof, Forschungsbericht Nr. 1879, München, July 30, 1943.

III. Tests for determination of the heat transfer coefficients at the blade profile

IV. Temperature distribution in the cross section of hollow turbine blades

V. Calculation of the thermal stresses

VI. Consideration of the effect of the radiation on the blade temperature

VII. Tests on blade segments and comparison with the calculation

VIII. Error of measurement in installing thermocouples in the air or gas flow

IX. Power requirement for cooling and prospects of the hollow-blade turbine

X. References

LIST OF SYMBOLS

Q	heat content (K cal/h)
λ	heat conductivity (K cal/m, °C, h)
ϑ	temperature, °C
T	absolute temperature, °K
f	blade cross section, meters^2
U	blade circumference, meters
α	heat transfer coefficient $\left(\text{K cal}/\text{m}^2, \text{°C}, \text{h}\right)$
G_K	weight of cooling air, kilograms per second
G_G	weight of gas, kilograms per second
c_p	specific heat (K cal/kg, °C)
Re	Reynolds number

Nu	Nusselt number
d	hydraulic diameter, meters
δ	wall thickness, meters
η	viscosity $\left(\text{kg-sec}/\text{m}^2\right)$
γ	specific weight, kilograms per meter^3
g	gravitational acceleration, meters per second^2
A	mechanical heat equivalent (m kg/K cal)
Ho	turbine gradient (K cal/kg)
u	circumferential velocity, meters per second
w_1	relative velocity in the turbine blade, meters per second
c_1	nozzle velocity, meters per second
z	number of blades
σ	stress, kilograms per millimeter^2
l	blade length, meters
D_m	diameter of a blade partition circle, meters
r	blade radius, meters
ω	angular velocity (1/sec)
t_s	blade spacing, meters

Subscripts:

i	cooling duct
a	blade profile
T	turbine
D	turbine nozzle
s	radiation

I. INTRODUCTION

For keeping high gas temperatures of 800° C to 900° C under control, various methods of blade cooling were applied since suitable materials with sufficient heat resistance do not exist. The cooling methods can be subdivided as follows:

1. Load cooling.- A part of the turbine rotor circumference is loaded with cooling air.

2. Root cooling.- The turbine disc and the rim, respectively, are cooled by special measures; thus heat is removed from the blade by conduction.

3. Internal cooling.- A hollow blade design is used and cooling air is made to flow through the interior.

The load cooling was successfully developed at the DVL. Leist [1][1] and Knoernschild [2] have made various reports on it. This kind of cooling has only a limited field of application. Like every other partially loaded turbine the load cooled turbine must be designed as a constant pressure turbine. Actual construction of a multistaged turbine of this type will be difficult.

By the root cooling the temperature in the highly stressed part of the blade can be lowered. Without connection with other types of cooling it is used only for short and wide blades and moderate gas temperatures (750° C to 800° C).

The internal cooling of the blade with air which is either precompressed or moved by the blades in star is the object of the present treatise. With this type of blade cooling, which is supported in its effect by the root cooling, high gas temperatures and circumferential velocities can be used. Also, a multistaged turbine can be designed without special difficulties when this type of cooling is used.

II. TEMPERATURE VARIATION AND STRESS ALONG THE BLADE WITH HEAT CONDUCTION TO THE ROTOR DISC

Heat Transfer Coefficients at the Blade

First, the heat transfer coefficients must be known for calculation of the blade temperatures. The heat transfer at the blade

[1]The brackets refer to the references.

profiles of the turbine rotor may be estimated according to figure 1 on the basis of the following empirical law.

If one selects as length of reference for the characteristic values Nu and Re the diameter of a circular tube of the same circumference as the blade one can calculate with the test results of the tube with a circular cylinder as cross section. The results for the heat-transfer coefficient of a plate also may be considered for comparison if one substitutes instead of the length of reference l the diameter of a circular tube with the same circumference $d = 2l/\pi$. The results for plate and cylinder plotted in figure 2 are obtained which will be used for calculation of the heat transfer at the blade profile.

The heat transfer between cooling air and internal blade wall can be calculated by introducing the hydraulic radius or diameter, respectively, of the cooling duct $d = 4f_k/U$, and using it as length of reference for the characteristic values Nu and Re. For the connection between Nu and Re the results for the heat transfer in the cylindric tube are assumed according to figure 3. With the aid of the above considerations the heat transfer coefficients may be determined.

The Magnitude of the Stagnation Temperature

The temperature of the gas ahead of the turbine nozzles is assumed to be ϑ_{gas}. In the nozzles the velocity c_1 is produced. The temperature at the exit of the nozzles amounts to $\vartheta_{gas} = H_{c1}/cp$. The relative velocity of the flow with respect to the blade is $w_1 = c_1 - u$. It is assumed that 85 percent of the velocity head $H_{w1} = w_1^2/2g$ are converted into heat at the stagnation point. One then obtains at the stagnation point the temperature

$$\vartheta_a = \vartheta_{gas} - \frac{H_{c1}}{cp} + 0.85\,\frac{H_{w1}}{cp} = \vartheta_{gas} - \Delta t$$

ϑ_a is designated as stagnation temperature and considered decisive for the heat transfer. Therefore the relation

$$\Delta t = \frac{A}{cp2g} c_1^2 \left[1 - 0.85 \left(\frac{w_1}{c_1} \right)^2 \right]$$

is valid for the difference between gas temperature and stagnation temperature. By means of the velocity triangle in figure 1 the following formulas can be derived for the ratio w_1/c_1:

$$\frac{w_1}{c_1} = \sqrt{1 - 2\frac{u}{c_1} \cos \alpha_1 + \left(\frac{u}{c_1} \right)^2}$$

The stagnation temperature corresponds to the temperature assumed by an uncooled blade. The factor 0.85 is a mean value which applies to constant pressure profiles. A thorough investigation on the magnitude of the stagnation temperature in uncooled blades was carried out by E. Eckert and Weise [3]. For a circumferential velocity of 250 meters per second the stagnation temperature is about 100° C lower than the gas temperature.

Blade Temperature Without Consideration of the Heat Conduction to the Blade Root

First a hollow blade is considered where no heat conduction to the rotor disc takes place. If one neglects, moreover, the temperature differences in the blade wall and designates the temperature of the internal and external surface with ϑ_o one obtains the following simple relation:

The heat content transferred by the hot gas at the external blade surface

$$Q_1 = \alpha_a U_a \left(\vartheta_a - \vartheta_o \right) dx$$

must equal the heat content transmitted to the cooling air at the internal circumference

$$Q_2 = \alpha_i U_i (\vartheta_o - \vartheta_i)\, dx$$

One thus obtains

$$\vartheta_o = \frac{\alpha_a U_a \vartheta_a + \alpha_i U_i \vartheta_i}{\alpha_a U_a + \alpha_i U_i}$$

or, referred to the stagnation temperature,

$$\frac{\vartheta_o}{\vartheta_a} = \frac{1 + \dfrac{\alpha_i}{\alpha_a} \dfrac{U_i}{U_a} \dfrac{\vartheta_i}{\vartheta_a}}{1 + \dfrac{\alpha_i}{\alpha_a} \dfrac{U_i}{U_a}}$$

ϑ_o represents the mean temperature of the cross section if the temperature differences in the cross section and the heat flow along the blade are neglected.

The formula shows that for a given gas temperature the blade temperature is dependent on the three following values only:

(1) Ratio of the heat transfer coefficients (α_i/α_a)

(2) Ratio of the blade circumferences (U_i/U_a)

(3) Ratio cooling air/stagnation temperature $(\vartheta_i/\vartheta_a)$

Blade Temperature with Consideration of the Heat Conduction to the Blade Root

The blade root and the rotor rim, respectively, have generally a lower temperature than the blade. Therefore a heat flow will take place along the blade toward the rotor disc. For the heat flow along the blade the relation

$$Q_4 - Q_3 = \frac{d}{dx}\left(\lambda f \frac{d\vartheta}{dx}\right) dx$$

is valid.

From the heat balance for the cross-hatched element (fig. 5) of the blade follows

$$Q_4 - Q_3 - Q_1 + Q_2 = 0$$

From the formula above then follows the differential equation

$$\frac{d}{dx}\left(\lambda f \frac{d\vartheta}{dx}\right) - \alpha_a U_a \left(\vartheta_a - \vartheta\right) + \alpha_i U_i \left(\vartheta - \vartheta_i\right) = 0$$

In this equation there may be at first f as well as U_a and U_i functions of x. If one considers at first the case of a cylindric hollow blade, therefore f = constant, U_a and U_i = constant, one obtains

$$\lambda f \frac{d^2\vartheta}{dx^2} - \alpha_a U_a \left(\vartheta_a - \vartheta\right) + \alpha_i U_i \left(\vartheta - \vartheta_i\right) = 0$$

One equates

$$\beta_a^2 = \frac{\alpha_a U_a}{\lambda f}$$

$$\beta_i^2 = \frac{\alpha_i U_i}{\lambda f}$$

There results

$$\frac{d^2\vartheta}{dx^2} - \left(\beta_a{}^2\vartheta_a - \beta_i{}^2\vartheta_i\right) + \left(\beta_a{}^2 - \beta_i{}^2\right)\vartheta = 0$$

If one further equates

$$\beta^2\vartheta_o = \left(\beta_a{}^2\vartheta_a + \beta_i{}^2\vartheta_i\right)$$

$$\beta^2 - \left(\beta_a{}^2 + \beta_i{}^2\right)$$

One obtains a differential equation which formally agrees with the differential equation for the temperature variation on an ordinary cylindric rod without internal cooling. The differential equation reads

$$\frac{d^2\vartheta}{dx^2} - \beta^2(\vartheta_o - \vartheta) = 0$$

and its solution

$$\vartheta_o - \vartheta = Ae^{\beta x} + Be^{-\beta x}$$

With the boundary conditions

(1) $x = 0 \qquad \vartheta = \vartheta_1$

(2) $x = l \qquad \left(\frac{d\vartheta}{dx}\right)_{x = l} = 0$

The second boundary condition expresses that the heat flow at the blade tip is neglected. One obtains the following equations for determination of the constants A and B

$$\vartheta_a - \vartheta_1 = A + B$$

$$0 = Ae^{\beta h} - Be^{-\beta h}$$

and the constants themselves

$$A = \left(\vartheta_o - \vartheta_1\right) \frac{e^{-\beta h}}{e^{\beta h} + e^{-\beta h}}$$

$$B = \left(\vartheta_o - \vartheta_1\right) \frac{e^{\beta h}}{e^{\beta h} + e^{-\beta h}}$$

The equation for the temperature variation along the blade finally reads:

$$\vartheta_o - \vartheta = \left(\vartheta_o - \vartheta_1\right) \frac{e^{\beta(x-h)} + e^{-\beta(x-h)}}{e^{\beta h} + e^{-\beta h}}$$

$$\vartheta_o - \vartheta = \left(\vartheta_o - \vartheta_1\right) \frac{\cot \beta(x - h)}{\cot \beta h}$$

For large values of βx, ϑ becomes $\vartheta = \vartheta_o$. For the blade tip $x = h$ generally the values βh become so large that the heat conduction can be neglected. Then . . . (symbol missing in the original) represents the temperature at the blade tip and at the same time the highest temperature occurring. In this case one may write in sufficient approximation

$$\vartheta_o - \vartheta = \left(\vartheta_o - \vartheta_1\right) e^{-\beta x}$$

This result corresponds to the assumption that ϑ_o represents the blade temperature for neglected heat conduction.

Derivation of a Formula for the Ratio of the Heat Transfer Coefficients

Since in the formulas for the blade temperatures ϑ_o there appears only the ratio α_i/α_a, a formula for it shall be derived. α_i/α_a represents a measure for the efficiency of the cooling.

In the region of Reynolds numbers which has to be considered for gas turbine blades the following equations are approximately valid for the Nusselt numbers:

$$Nu_i = \frac{\alpha_i\, d_i}{\lambda_i} = C_i Re_i^{\,m} = 0.0342 Re_i^{0.735}$$

$$Nu_a = \frac{\alpha_a\, d_a}{\lambda_a} = C_a Re_a^{\,m} = 0.0666 Re_a^{0.735}$$

Nu_i is assumed valid for the internal duct, Nu_a for the heat transfer at the external surface of the blade. Therefrom one obtains the following expression for the ratio

$$\frac{\alpha_i}{\alpha_a} = \frac{\lambda_i}{\lambda_a}\frac{d_a}{d_i}\left(\frac{C_i}{C_a}\right)\left(\frac{Re_i}{Re_a}\right)^m$$

The Reynolds number can be written $Re = w\, d\gamma/\eta g$; therewith one obtains for the ratio

$$\frac{Re_i}{Re_a} = \frac{w_i\ d_i\gamma_i}{\eta_i g}\ \frac{\eta_a g}{w_a\ d_a\gamma_a}$$

Furthermore, the weight flow per second is $G = w\gamma F$ or $w\gamma = \frac{G}{F}$. Thus one obtains

$$\frac{Re_i}{Re_a} = \frac{G_K f_{gas}}{f_K G_{gas}}\ \frac{d_i}{d_a}\ \frac{\eta_a}{\eta_i}$$

If one designates the axial projection of the nozzle area by F,

$$F = \pi\, D_m h \epsilon$$

with ϵ taking the narrowing by the finite blade thickness into consideration.

The cross section through which the gas flows then is

$$f_{gas} = F \sin \beta_1$$

The following formulations are used for the viscosity and the heat conductivity:

$$\eta = \eta_o \left(\frac{T}{T_o}\right)^{0.69}$$

$$\lambda = \lambda_o \left(\frac{T}{T_o}\right)^{0.69}$$

Then there becomes

$$\frac{\eta_a}{\eta_i} = \left(\frac{T_a}{T_i}\right)^{0.69}$$

$$\frac{\lambda_i}{\lambda_a} = \left(\frac{T_i}{T_a}\right)^{0.69}$$

The ratio cooling air weight/gas weight is designated by p.

$$p = \frac{G_K}{G_{gas}}$$

Therewith one obtains

$$\frac{Re_i}{Re_a} = p\frac{F_{sm}\beta_1}{F_K}\frac{\alpha_i}{\alpha_a}\left(\frac{T_a}{T_i}\right)^{0.69}$$

and finally for

$$\frac{\alpha_i}{\alpha_a} = \frac{\lambda_i}{\lambda_a}\frac{d_a}{d_i}\frac{C_i}{C_a}\left(\frac{Re_i}{Re_a}\right)^m$$

$$= \left(\frac{T_i}{T_a}\right)^{0.69}\frac{d_a}{d_i}\frac{C_i}{C_a}p^m\left(\frac{F_{sm}\beta}{F_K}\right)^m\left(\frac{d_i}{d_a}\right)^m\left(\frac{T_a}{T_i}\right)^{0.69m}$$

$$\boxed{\frac{\alpha_i}{\alpha_a} = 0.514\left(\frac{F_{sm}\beta}{F_K}\right)\left(\frac{d_a}{d_i}\right)^{0.265}\left(\frac{T_i}{T_a}\right)^{0.183}p^m}$$

The cooling air cross section of the rotor is $F_K = z \cdot f_K$, with f_K designating the cross section of the cooling duct of a blade and z designating the number of blades of the turbine rotor. The ratio gas cross section/cooling air cross section F/F_K can be transformed as follows:

$$\frac{F}{F_K} = \frac{\pi D_m h \epsilon}{z f_K} = \frac{z t_s h \epsilon}{z f_K}$$

$t_s h$ is the nozzle area corresponding to one rotor blade. The equation for α_i/α_a shows clearly the separate effects of the dimensions, the temperatures, and the "referred" cooling air quantity. The term with the temperatures T_i/T_a has an exponent 0.133. One can see that the influence of the temperatures on α_i/α_a is not very essential. It is noteworthy that the magnitude of the absolute pressure does not appear in the formula, which means that the pressure does not affect the merit of the cooling. Neither is the influence of the term with d_a/d_i very decisive. The term with F/F_K, on the other hand, is essential.

Favorable factors for the cooling are therefore

(1) Wide blade spacing, that is, small number of blades

(2) Small cooling duct cross section, that is, narrow blades

(3) Large nozzle height, that is, large blade length

For geometrically similar turbines no changes occur in the ratios F/F_K and d_a/d_i. Thus the merit of the cooling is the same for a large and a small turbine.

The ratio α_i/α_a is therefore, for a given blade shape, no function other than of the "referred" cooling air weight p. Therewith α_i/α_a also is no longer dependent on anything but p. This result simplifies the investigations by calculation very essentially.

Centrifugal Force Stress of the Turbine Blade.

The stresses caused by the centrifugal forces are first ascertained for a cylindric blade. The centrigual force of the blade of the length x, according to figure 6, is:

$$C = \int_0^x \frac{\gamma}{g} \omega^2 fr \, dx = \frac{\gamma}{g} \omega^2 f \int_0^x r \, dx$$

With $r = R - x$ the integral becomes

$$\int_0^x r \, dx = \int_0^x (R - x) \, dx = Rx - \frac{x^2}{2}$$

Thus the centrifugal stress becomes

$$\sigma = \frac{c}{f} = \frac{\gamma}{g} \omega^2 R^2 \left(\frac{x}{R} - \frac{x^2}{2R^2} \right)$$

The maximum stress at the blade root, therefore for $x = l$, becomes

$$\sigma_l = \frac{\gamma}{g} \omega^2 \left(Rl - \frac{l^2}{2} \right) = \frac{\gamma}{g} \omega^2 l \left(R - \frac{l}{2} \right)$$

and with $R_m = R - l/2$, σ_l becomes

$$\sigma_l = \frac{\gamma}{g} \omega^2 R_m^2 \frac{l}{R_m} = \frac{\gamma}{g} u_m^2 \frac{l}{R_m}$$

The stress $\sigma_o = \gamma / g u_m^2$ is designated as circumferential stress. That is, the stress appearing in a thin ring rotating with u_a. Thus the maximum stress in a cylindric blade is

$$\sigma_l = \frac{l}{R_m} \sigma_o$$

For the stress variation along the cylindric blade the equation

$$\sigma = \sigma_o\left(\frac{x}{R} - \frac{x^2}{2R^2}\right) = \sigma f_1\left(\frac{x}{R}\right)$$

is valid. The function $f_1(x/R)$ is plotted in figure 7.

For a tapered blade, according to figure 8, which ends in a point, the stress can be calculated as follows:

The cross section at an arbitrary location is

$$f = \frac{f_1}{x_1}x = Kx$$

The centrifugal force of the blade of the length x is therefore

$$C = \frac{\gamma}{g}\omega^2 \int_0^x Kx(R - x)\,dx = \frac{\gamma}{g}\omega^2 K\left(R\frac{x^2}{2} - \frac{x^3}{3}\right)$$

The stress at the location x then results as

$$\sigma' = \frac{C}{f} = \frac{\frac{\gamma}{g}\omega^2 K\left(R\frac{x^2}{2} - \frac{x^3}{3}\right)}{Kx} = \frac{\gamma}{g}\omega^2 R^2\left(\frac{x}{2R} - \frac{x^2}{3R^2}\right)$$

and with $u^2 = \omega^2 R^2$ and $\gamma/gu^2 = \sigma_o$, σ becomes

$$\sigma = \sigma_o\left(\frac{x}{2R} - \frac{x^2}{3R^2}\right) = \sigma_o f_2\left(\frac{x}{R}\right)$$

This formula for σ' signifies that the stress in the linearily tapered blade is independent of the degree of taper k. If one cuts off the point of the blade (fig. 8) considered before, the centrifugal force in each section is smaller by the centrifugal force of the point. This latter is

$$C_2 = \sigma_2 f_2 = \Delta\sigma f$$

The change in stress by the elimination of the point amounts to

$$\Delta\sigma = \sigma_2 \frac{f_2}{f}$$

With $f_2/f = x_2/x$ one obtains

$$\Delta\sigma = \sigma_2 \frac{x_2}{x} = \sigma_o f_2 \left(\frac{x_2}{R}\right) \frac{x_2}{x}$$

Thus the centrifugal stress in the trapezoidal blade with the cross sections f at the root and f_2 at the external diameter becomes

$$\sigma = \sigma - \Delta\sigma = \sigma_o \left[f_2 \left(\frac{x}{R}\right) - \frac{x_2}{x} f_2 \left(\frac{x_2}{R}\right) \right]$$

The function $f_2\left(\frac{x}{R}\right) = \left(\frac{x}{2R} - \frac{x^2}{3R^2}\right)$ is plotted in figure 9 and is generally valid for the calculation of the stress in a linearily tapered blade.

Calculation of the Temperature and the Stress in Two Model Hollow Blades

Following the basic calculations given above for temperatures and stresses of two blades (fig. 10) with different shapes of the cross section the cooling duct will be determined. The blade edges of the blade H5 do not come directly into contact with the coolant. The shape of the cooling duct depends on the method of production. The blade is partitioned at the center and the duct is made by milling in each half. The two blade halves then are welded together. The disadvantages of this method, uneven temperature distribution and thermal stresses, are discussed in detail in chapter 3 and 4. The blade form H7 has everywhere equal wall thickness and correspondingly short paths of heat flow and therefore uniform temperature distribution. For the calculation example the operating data are assumed in table I. The dimensions of the blades used in the calculation examples are given in table II.

With the values indicated in tables I and II one calculates the factors contained in the equation for α_i/α_a according to table III.

The ratio α_i/α_a for the two blades H5 and H7 is plotted as a function of the cooling air mass in figure 11.

The blade temperature ϑ_o at the point of the blade results from the equation

$$\frac{\vartheta_o}{\vartheta_a} = \frac{1 + \frac{\alpha_i}{\alpha_a}\frac{U_i}{U_a}\frac{\vartheta_i}{\vartheta_a}}{1 + \frac{\alpha_i}{\alpha_a}\frac{U_i}{U_a}}$$

The values calculated from it are represented in figure 12 for a gas temperature of 900°.

One can see that for the blade H7 the cooling air requirement for the same blade temperature is essentially smaller. For a blade temperature of 650° the requirements are

For the blade H5 - 7.6 percent cooling air

For the blade H7 - 4.0 percent cooling air

The more favorable values for the blade H7 can be traced back mainly to the larger ratio U_i/U_a. The temperature variation is obtained from the equation

$$\vartheta_o - \vartheta = \left(\vartheta_o - \vartheta_1\right) e^{-\beta x}$$

For the value β the relation

$$\beta = \sqrt{\frac{\alpha_a U_a \left(1 + \frac{\alpha_i}{\alpha_a}\frac{U_i}{U_a}\right)}{\lambda f}}$$

is valid, with α_a being determined from Re_a and Nu_a. The missing values are contained in table IV.

In figures 13 and 14 the temperatures and stresses for the blade H5 are plotted. For the temperature at the root ϑ_1 400° and 500° were assumed. The stresses are plotted for a circumferential velocity of 250 meters per second.

For the blade H7 the stresses are represented also for a circumferential velocity of 300 meters per second. (See figs. 15 and 16.)

The temperatures change with the circumferential velocity. The stagnation temperature decreases because a larger gradient is converted in the nozzle for equal u/c_1. Accordingly one obtains for $u = 300$ meters per second smaller blade temperatures and thus a larger permissible stress. The fatigue strength of the material is regarded as decisive for the permissible stress. In figures 13 to 16 the fatigue strengths σ_D corresponding to the various blade temperatures are plotted. The material "Böhler SAS 8" with the σ_D - values according to figure 17 was used.

The difference between the blade stress σ in a blade section and the permissible stress σ_D is called reserve stress. The minimum reserve stress appears in the critical cross section and amounts for instance according to figure 16 for $u = 300$ meters per second to about 7 kilograms per millimeter^2. The results of the

calculation show that for the hollow blade H7 circumferential velocities of more than 300 meters per second are permissible which was confirmed by test stand experiments.

After the example above the blade H7 is to be examined for various other circumferential velocities. Under the assumption of similar velocity triangles, that is, u/c_o = constant, the gradient converted in the turbine stage is, as already mentioned, a function of the circumferential velocity. The stagnation temperature increases for a small circumferential velocity, because the temperature drop in the nozzle is smaller. For a gas temperature of 900° C one obtains for various circumferential velocities the following stagnation temperatures:

Circumferential velocity, m/sec	150	200	250	300
Stagnation temperature, C	866	840	804	763

One can see that for a circumferential velocity of u = 150 meters per second the stagnation temperature is about 100 percent higher than for 300 meters per second. The centrifugal stress in the blade increases with the circumferential velocity whereas the blade temperature decreases. The influence of the temperature is so large that the difference between fatigue strength and stress remains almost constant, independent of the circumferential velocity.

In figure 18 the reserve strength in the critical cross section, that is, the difference between fatigue strength and stress at the blade location subject to maximum stress is plotted versus the circumferential velocity. The reserve strength increases for the same percent cooling air mass, between 300 and 150 meters per second only from 6.1 to 7.3 kilograms per millimeter^2 whereas the centrifugal stress at the root of the blade decreases from 17 kilograms per millimeter^2 to 4.2 kilograms per millimeter^2. One can see from these numerical values that a gas turbine blade may be operated with almost the same safety with respect to break for large as for small circumferential velocity. The heat gradient used in the turbine stage is essential for the reserve strength.

TESTS FOR DETERMINATION OF THE HEAT TRANSFER COEFFICIENT AT THE BLADE PROFILE

Justification for the test method.- The tests carried out on blade segments for actual conditions unchanged with respect to temperature and dimensions confirmed essentially the assumptions on

the heat transfer coefficients as they were obtained from the comparison of the blade profile with the cylindric tube and the plate in a longitudinal flow. A satisfactory installation of the thermocouples on the small gas turbine blades of 16 to 20 millimeter widths and wall thicknesses below 1 millimeter is extremely difficult. For this reason, the heat transfer coefficients were measured on an enlarged blade model. It is known that the heat transfer coefficient or the Nusselt number, respectively, is independent of the direction of the heat flow. It is therefore a matter of indifference whether the blade profile absorbs or gives off heat. Thus the measurements were made on an electrically heated model. A wind tunnel designed for flow investigations by the author (fig. 19) was used.

Description of the test arrangement.- In an existing blade cascade with three test blades the center blade was replaced by an electrically heated aluminum blade. The blade profile used for the measurements corresponds to the blade H3 indicated in table II. The blade width was increased from 16 millimeters on the original blade to 100 millimeters on the model blade.

A photograph of the blade cascade with the rectangular wooden nozzle is presented in figure 20. One can see the thermowires led sideways to the switch by which the individual test points can be connected with the indicator. The test blade with the thermowires and the connection clamps for heating is reproduced in figure 21. Ten temperature test points are arranged in each of the two cross sections of the test blade.

The installation of the thermocouples and the location of the three heating rods can be seen from figure 22.

Bore holes were provided near the surface into which the thermocouples are introduced from the outside. The soldering joints of the thermowires were then rigidly connected with the blade by means of a small screw. In view of heat conductivity such a type of blade material was selected that a uniform temperature distribution in the cross section could be expected; the test results confirmed this expectation.

The wind tunnel (fig. 19) consists of a radial blower driven by about 10 PS (German HP) motive power which feeds into a wooden settling chamber. A well rounded nozzle is arranged on the side opposite the air inlet. The nozzle must be adjustable because a different nozzle height corresponds to each flow incidence β_1 of the cascade. The blower can be regulated by a butterfly valve

installed on the side of the inlet. By adjustment of the butterfly valve a certain excess pressure can be adjusted in the chamber.

Test procedure and evaluation.- The free-stream velocity of the blade cascade was ascertained from the pressures as follows. Since according to experience the pressure conversion in a well rounded nozzle takes place practically without losses, the velocity in the nozzle can be determined from the difference between the chamber pressure and the static pressure in the nozzle. Thus the velocity in the nozzle is

$$w_1 = \sqrt{\frac{2g}{\gamma} \Delta p}$$

for the pressure drop Δp one has to insert

$$\Delta p = p_{boiler} - p_{nozzle} \text{ mmWS}$$

In the following table, for instance, the measured values for a nozzle angle of $40^{\circ}35'$ are compiled.

Since for the same nozzle angle a certain nozzle pressure is coordinated to each boiler pressure, the velocity can also be given as a function of the boiler pressure. In figure 23 the velocity w_1 is plotted for three nozzle angles as a function of the chamber pressure. Then for the temperature measurements only a certain boiler pressure was adjusted and the pertaining velocity taken from the chart.

The center blade was electrically heated by three heating rods. The heating power was determined by measurement of amperage and voltage. In the tests one adjusted a certain boiler pressure, waited for the equilibrium condition of the temperatures and then read the 20 temperature test points. The power required for heating is

$$Q = \frac{0.2386}{1000} UI \text{ kcal/sec}$$

The heating power corresponds to the supplied heat quantity and, for equilibrium condition, must equal the heat content taken away by the air stream. Thus

$$Q = \alpha_a F_o \Delta\vartheta \frac{1}{3600} \text{ kcal/sec}$$

with $\Delta\vartheta$ indicating the mean difference between wall temperature and air temperature. Since the differences in wall temperature are small, the arithmetic mean of the wall temperatures was used for the calculation. This procedure is justified because the individual test points are spaced almost evenly over the circumference of the profile. To be exact, the mean temperature should be calculated from the following expression:

$$\vartheta_{w_{mean}} = \frac{\int \vartheta_w \, d_s}{d_s} = \frac{\sum \vartheta_w \Delta_s}{z \, \Delta_s}$$

If all test point distances are equal, the mean value will of course equal the arithmetic mean value of the temperatures, thus

$$\vartheta_{w_{mean}} = \frac{\sum \vartheta_w}{z}$$

z is the number of the test points on the circumference of the profile. The blade surface is

$$\text{Circumference} \times \text{Blade length},$$

therefore

$$F_o = U_a l = 272.5 \times 300 = 0.08175 \text{ m}^2$$

In calculating the dimensionless characteristic values Re and Nu values for the temperature of the outside flow or of the air in the boiler, respectively, are substituted.

The Reynolds number is

$$Re = \frac{w_1 \, d_a}{\gamma}$$

The length of reference d_a is determined from the profile circumference as follows:

$$d_a = \frac{U_a}{\pi} = 86.8 \text{ mm}$$

For the velocity the free-stream velocity of the blade, that is, the velocity in the nozzle, is inserted. The Nusselt number is

$$Nu = \frac{\alpha_a \, d_a}{\gamma}$$

The value determined from power required for heating and temperature difference is substituted for the heat transfer coefficient α_a. The tables VI and VII show the test values for pressure and temperatures for a nozzle angle of $40^\circ 35'$.

The measured dimensionless values Nu and Re are plotted in figure 24. The Reynolds number is between 10^5 and 2.5×10^5, therefore in the turbulent region. The values measured for the three nozzle angles lie very close to the straight line for the mean value of cylinder and plate. The deviations are less than 10 percent.

It is remarkable that a larger Reynolds number results for the same Nusselt number for a small nozzle angle (30°). To a smaller nozzle angle corresponds a larger deflection of the flow and thus a larger lift coefficient. It is known from wing tests that the heat transfer increases with growing lift coefficient. Here the

reversed influence can be seen. If one attempts to introduce in the Reynolds number the exit velocity w_2 one obtains, it is true, the usual influence of the deflection or the lift coefficient, respectively, but the test values are in no better position with respect to the calculated curve of comparison for cylinder and plate. Thus the free-stream velocity w_1 is used thereafter in the calculations.

For the investigated profile the velocity ahead of and behind the cascade is not very different. It is presumed that for profiles where a large change in velocity occurs, as in excess pressure profiles, the calculation must be made with a mean value of the velocity.

IV. TEMPERATURE DISTRIBUTION IN THE CROSS SECTION OF HOLLOW TURBINE BLADES

The mean temperature of a blade cross section, where the root cooling takes effect no longer, was designated by ϑ_o. This temperature actually appears only when the heat flow from the internal to the external circumference takes place without a noteworthy drop in temperature. ϑ_o is therefore only a mean value; actually a temperature drop occurs in the blade wall and the temperature is not evenly distributed over the cross section.

The Minimum Temperature in the Blade Cross Section

A hollow blade with a corss section according to figure 25 is considered. The center part of the blade between C and C' is naturally cooled more effectively than the blade edges. Thus the minimum temperature of the cross section will appear in the core of the blade at A and D. One obtains the approximate minimum temperature in the cross section $\vartheta_{o_{min}}$, if one takes the fact into consideration that for a straight part of the blade wall, internal and external circumference are equal. If one substitutes accordingly in the formula the value $U_i = U_a$ for ϑ_o, one obtains

$$\vartheta_{c_{min}} = \vartheta_a \frac{1 + \frac{\alpha_i}{\alpha_a} \frac{\vartheta_i}{\vartheta_a}}{1 + \frac{\alpha_i}{\alpha_a}}$$

Temperature Variation in the Blade Edges

In the blade edges the heat content entering from the outside is not directly given off to the cooling air, as in the middle part of the blade wall. The heat content entering at B must first flow to C and can only there be transferred to the cooling air. The heat flow from B to C causes an accordingly large difference in temperature.

By way of calculation, the temperature variation can be determined as follows: One considers first the heat flow in the blade edges between B and C in figure 26. The change of the heat flow in the cross hatched element (fig. 26) must equal the heat absorbed from the outside by heat transfer. These circumstances are represented by the following equations

$$Q_1 - Q_2 = 2Q_3$$

$$\frac{d}{dx}\left(\lambda l \frac{d\vartheta}{dx} dx\right) = \alpha_a \left(\vartheta_a - \vartheta\right) 2 \, dx$$

If one designates $\vartheta - \vartheta_a = \theta$, one obtains the differential equation

$$l \frac{d^2\theta}{dx^2} - \frac{dl}{dx} \frac{d\theta}{dx} - 2 \frac{\alpha_a}{\lambda} \theta = 0$$

For the cross section decreasing linearily was substituted

$$l = 2 \times \tan \varphi$$

Thus there resulted finally the differential equation

$$\frac{d^2\theta}{dz^2} + \frac{1}{z}\frac{d\theta}{dz} - \frac{\theta}{z} = 0$$

in which

$$z = \frac{\alpha_a}{\lambda \tan \varphi} x$$

or

$$z = b^2 x$$

This equation is a Bessel differential equation of zero order the solution of which reads:

$$\theta = AI_o\left(2i\sqrt{z}\right) - BN_o\left(2i\sqrt{z}\right)$$

In order to have θ become real, B must equal zero.

For $x = x_1$, $z = z_1$ and $\vartheta = \vartheta_1$. Therefrom follows

$$A = \frac{\vartheta_1 - \vartheta_a}{I\left(2i\sqrt{z_1}\right)}$$

The temperature variation in the blade edge is therefore represented by the equation

$$\vartheta - \vartheta_a = \left(\vartheta_1 - \vartheta_a\right) \frac{I_o\left(2i\sqrt{z}\right)}{I_o\left(2i\sqrt{z_1}\right)}$$

Temperature Variation in the Blade Wall

The temperature variation in the blade wall can be ascertained in the following manner. The heat

$$Q_1 = \alpha_a \left(\vartheta_a - \vartheta \right) dx$$

enters from the outside into the crosshatched element (fig. 27). Due to heat conduction, there enters from C

$$Q_2 = \lambda \frac{d(\vartheta x)}{dx} \vartheta$$

In direction towards A,

$$Q_3 = \lambda \frac{d(\vartheta x' + dx)}{dx} \vartheta$$

leaves the element. The heat content which on the inside is absorbed by the air is

$$Q_4 = \alpha_i \left(\vartheta - \vartheta_i \right) dx$$

The temperature difference perpendicular to the blade wall was neglected here.

One can transform the expression $\frac{d(\vartheta x' + dx)}{dx}$ as follows:

$$\frac{d(\vartheta x' + dx)}{dx} = \frac{d}{dx} \left(\vartheta - \frac{d\vartheta}{dx} \right) = \frac{d\vartheta}{dx} + \frac{d^2\vartheta}{dx^2} dx$$

The heat balance for the element is

$$Q_1 + Q_2 - Q_3 - Q_4 = 0$$

$$\alpha_a\left(\vartheta_a - \vartheta\right) dx + \lambda \frac{d\vartheta}{dx} \vartheta - \lambda \left(\frac{d\vartheta}{dx} - \frac{d^2\vartheta}{dx^2} dx\right) \vartheta - \alpha_i\left(\vartheta - \vartheta_i\right) dx$$

therefrom follows

$$\lambda \vartheta \frac{d^2\vartheta}{dx^2} - \vartheta\left(\alpha_i + \alpha_a\right) + \alpha_a \vartheta_a + \alpha_i \vartheta_i = 0$$

According to the formula above, $\vartheta_{o_{min}}$ is

$$\vartheta_{o_{min}}\left(\alpha_i + \alpha_a\right) = \vartheta_i \alpha_i + \vartheta_a \alpha_a$$

One equates $\alpha_i + \alpha_a = \alpha$ and $\frac{\alpha}{\lambda \vartheta} = a^2$; then the differential equation assumes the following shape:

$$\frac{d^2\vartheta}{dx^2} - a^2\left(\vartheta - \vartheta_{o_{min}}\right) = 0$$

The solution is

$$\vartheta - \vartheta_o = Ae^{ax'} + Be^{-ax'}$$

In the section C

$$x' = 0 \qquad \vartheta = \vartheta_1$$

At large distance from C

$$x' = \infty \qquad \vartheta = \vartheta_{o_{min}}$$

From the second condition there follows $A = 0$.

Thus the temperature variation in the part CA of the blade is represented by the equation

$$\vartheta - \vartheta_{o_{min}} = \left(\vartheta_1 - \vartheta_{o_{min}}\right)e^{-ax'}$$

Calculation of the Temperature at the Junction of the Blade Edge and the Blade Wall

The temperature ϑ_1 at the point C, the junction of the blade edge and the blade wall, is still unknown in the equations for the temperature variation. This temperature results from the condition that the heat flow must not change at this point. Therefore

$$\underbrace{2\lambda\left(\frac{d\vartheta}{dx}\right)_{x'=0}}_{\text{Heat flow in the blade wall}} = \underbrace{\lambda_1\left(\frac{d\vartheta}{dx}\right)_{x=x_1}}_{\text{Heat flow at the end of the blade edge}}$$

For the blade wall there was

$$\vartheta - \vartheta_o = \left(\vartheta_1 - \vartheta_{o_{min}}\right)e^{-ax'}$$

For $x' = 0$ there becomes

$$2\vartheta\left(\frac{d\vartheta}{dx}\right)_{x'=0} = 2\vartheta a\left(\vartheta_1 - \vartheta_{o_{min}}\right)$$

For the blade edge there becomes

$$\vartheta_1\left(\frac{d\vartheta}{dx}\right)_{x=x_1} = \vartheta_1\left(\vartheta_1 - \vartheta_a\right)\frac{iI\left(2i\sqrt{z_1}\right)}{I_o\left(2i\sqrt{z_1}\right)}\frac{b^2}{\sqrt{z}}$$

By equating the two expressions one obtains, if

$$A = \sqrt{2\,\frac{\vartheta}{\vartheta_1}\,\frac{\alpha_a}{\alpha}}$$

and

$$B = \frac{iI_1\left(2i\sqrt{z_1}\right)}{I_o\left(2i\sqrt{z_1}\right)}$$

are introduced,

$$\vartheta_1 = \frac{A\vartheta_{o_{min}} + B\vartheta_a}{A + B}$$

Maximum Temperature in the Blade Cross Section

The temperature variation in the blade edge is represented by the following equation

$$\vartheta - \vartheta_a = \left(\vartheta_1 - \vartheta_a\right) \frac{I_o\left(2i\sqrt{z}\right)}{I_o\left(2i\sqrt{z_1}\right)}$$

In this formula the temperature at the junction point C is known so that the variation of ϑ can be determined.

The maximum temperature at the point B is obtained if in the formula above the value z_2 is substituted for z. Therefore,

$$\vartheta_{max} - \vartheta_a = \left(\vartheta_1 - \vartheta_a\right) \frac{I_o\left(2i\sqrt{z_2}\right)}{I_o\left(2i\sqrt{z_1}\right)}$$

By means of the formulas given above the temperature at any point of the blade can be calculated if gas and cooling air temperature and the heat transfer coefficients are known.

Temperature Drop in the Blade Wall

In the calculation of the temperature of the blade wall at A the temperature drop perpendicular to the wall was neglected and internal and external wall temperature were assumed equal. Now the temperature drop in the wall is to be calculated.

An element of the length dx and the height 1 is considered. The heat quantity entering the element amounts to

$$Q = \alpha_a \left(\vartheta_a - \vartheta_I\right) dx$$

The heat content leaving it is

$$Q = \alpha_i \left(\vartheta_{II} - \vartheta_i\right) dx$$

$$\vartheta - \vartheta_a = \left(\vartheta_1 - \vartheta_a\right) \frac{I_o\left(2i\sqrt{z}\right)}{I_o\left(2i\sqrt{z_1}\right)}$$

his formula the temperature at the junction point C is known hat the variation of ϑ can be determined.

The maximum temperature at the point B is obtained if in the ula above the value z_2 is substituted for z. Therefore,

$$\vartheta_{max} - \vartheta_a = \left(\vartheta_1 - \vartheta_a\right) \frac{I_o\left(2i\sqrt{z_2}\right)}{I_o\left(2i\sqrt{z_1}\right)}$$

eans of the formulas given above the temperature at any point ne blade can be calculated if gas and cooling air temperature the heat transfer coefficients are known.

Temperature Drop in the Blade Wall

In the calculation of the temperature of the blade wall at A emperature drop perpendicular to the wall was neglected and rnal and external wall temperature were assumed equal. Now emperature drop in the wall is to be calculated.

An element of the length dx and the height 1 is considered. eat quantity entering the element amounts to

$$Q = \alpha_a \left(\vartheta_a - \vartheta_I\right) dx$$

eat content leaving it is

$$Q = \alpha_i \left(\vartheta_{II} - \vartheta_i\right) dx$$

The heat flow perpendicular to the wall causes a temperature gradient in the direction z, therefore

$$Q = -\lambda \frac{d\vartheta}{dz}\,dx = -\lambda \frac{\vartheta_I - \vartheta_{II}}{\delta}\,dx = -\frac{\lambda}{\delta}\Delta\vartheta$$

The calculation of $\Delta\vartheta$ is made as follows:

$$\alpha_i \vartheta_{II} - \alpha_i \vartheta_i = \frac{\lambda}{\delta}\Delta\vartheta$$

$$\vartheta_{II} = \vartheta_I - \Delta\vartheta = \frac{1}{\alpha_i}\left(\frac{\lambda}{\delta}\Delta\vartheta + \alpha_i\vartheta_i\right)$$

$$\vartheta_I = \frac{1}{\alpha_i}\left(\frac{\lambda}{\delta}\Delta\vartheta + \alpha_i\vartheta_i\right) + \Delta\vartheta$$

there is further

$$\alpha_a \vartheta_a - \alpha_a \vartheta_I = \frac{\lambda}{\delta}\Delta\vartheta$$

If one substitutes in this equation the calculated expression for ϑ_I, there results

$$\alpha_a \vartheta_a - \alpha_a\left[\frac{1}{\alpha_i}\left(\frac{\lambda}{\delta}\Delta\vartheta + \alpha_i\vartheta_i\right) + \Delta\vartheta\right] - \frac{\lambda}{\delta}\Delta\vartheta = 0$$

$$\alpha_a \vartheta_a - \alpha_a \vartheta_i = \Delta\vartheta\left(\frac{\alpha_a}{\alpha_i}\frac{\lambda}{\delta} + \alpha_a + \frac{\lambda}{\delta}\right)$$

therefore finally

$$\Delta\vartheta = \frac{\vartheta_a - \vartheta_i}{1 + \frac{\lambda}{\delta}\left(\frac{1}{\alpha_i} + \frac{1}{\alpha_a}\right)}$$

or, divided by ϑ_a,

$$\frac{\Delta\vartheta}{\vartheta_a} = \frac{1 + \frac{\vartheta_i}{\vartheta_a}}{1 + \frac{\lambda}{\delta}\left(\frac{1}{\alpha_i} + \frac{1}{\alpha_a}\right)}$$

Graphical Supplement of the Temperature Field

Naturally the variation of the temperatures determined by calculation represents only an approximation. To be exact, one is dealing with a temperature field, therefore with a two-dimensional problem. The calculated temperatures at the points A, B, and C form as it were the scaffold for the temperature field. The temperature field must be a square net; such a net can be completed graphically by trial and error [4]. The heat flow per unit area is given by the equation (basic equation of heat conduction)

$$q_n = -\lambda \frac{d\vartheta}{dn} = -\lambda \frac{\Delta\vartheta}{\Delta n}$$

The heat quantity which flows through the length Δs (fig. 28) between the streamlines drawn in dashed lines, amounts to

$$\Delta Q = \lambda \frac{\Delta\vartheta}{\Delta n} \Delta s$$

An equal heat content must enter at the external surface on the length Δo. The average temperature at the surface is

$$\vartheta_m = \frac{1}{2}(\vartheta + \vartheta + \Delta\vartheta) = \vartheta + \frac{1}{2}\Delta\vartheta$$

The heat transfer coefficient is assumed to be α_a and the gas temperature ϑ_a. Then

$$\Delta Q = \alpha_a\left(\vartheta_a - \vartheta\right)\Delta o$$

If one takes $\sin\alpha = \frac{\Delta s}{\Delta o}$ into consideration, one obtains

$$\sin\alpha = \frac{\Delta s}{\Delta o} = \frac{\alpha_a\left(\vartheta_a - \vartheta_m\right)}{\lambda\frac{\Delta\vartheta}{\Delta n}}$$

The correctness of the temperature field that was drawn can be tested by means of the relation above.

For a hollow blade H8 the temperature field in the blade cross section was completely determined. (See fig. 30.) The operating conditions for this blade are particularly unfavorable. The blade operates with excess pressure ahead of the nozzles whereas for the other examples there is atmospheric pressure ahead of the nozzles and low pressure behind the nozzles. For the blade H8 there result, due to the large gas density, especially large heat transfer coefficients and larger temperature differences than for the other examples mentioned. First, the temperatures ϑ_o, ϑ_{ol}, ϑ_{min}, and ϑ_{max} were determined and moreover the temperature variation in the rib-like blade edge calculated. This "scaffold" was then completed by construction of a square net and controlled by the surface condition.

Heat Transfer at the Stagnation Point of the Blade

A mean heat transfer coefficient was used at first for the calculation of the temperature distribution in the blade cross

section. No exact data exist on the exact variability of this coefficient along the circumference. However, an estimate for the stagnation point of the profile can be made in the following manner.

It is known that the heat transfer at the stagnation point of a streamlined body depends only on the radius of curvature at this point. Test values on the magnitude of the heat transfer at the stagnation point of a cylinder have been compiled [5]. A formula given by Squire reads:

$$Nu = 1.01\sqrt{Re}$$

The values calculated with this formula agree well with the test results. For Reynolds numbers of 10^4 the heat transfer at the stagnation point is about twice as large as the average heat transfer. For $Re = 10^5$ both heat transfer coefficients are about equal. If one considers a blade profile with $d_a = 22$ millimeters and a diameter of curvature at the leading edge of 2.2 millimeters, the Reynolds number for the leading edge is, for $Re_a = 10^5$, $Re_1 = 10^4$ and one obtains the following Nusselt numbers:

$$Nu_a = 330$$

$$Nu_1 = 100$$

Therewith $\frac{a}{a_1}$ becomes

$$\frac{\alpha_a}{\alpha_{a_1}} = \frac{Nu_a \alpha_1}{\alpha_a Nu_1} = \frac{330 \times 2.2}{22 \times 100} = 0.33$$

Thus a heat transfer coefficient at the stagnation point on the leading edge 3.0 times as large as the mean heat transfer coefficient results for the case above. Due to the large heat transfer coefficients for slight rounding of the leading edge high temperatures appear there. It is therefore useful, to round the leading edges of gas-turbine blades sufficiently.

Calculation of the Maximum, Mean, and Minimum Temperature in the Blade Cross Section

By means of the formulas given above the maximum and minimum temperatures in the blade cross section can be determined and represented as

$$\frac{\vartheta_{o\min}}{\vartheta_a}$$

and

$$\frac{\vartheta_{o\max}}{\vartheta_a}$$

as functions of the cooling-air quantity. For the hollow blade H3 (dimensions according to table II) the values above are plotted in figure 31. The maximum temperature difference appearing in the blade section is found to be

$$\Delta t_{max} = \vartheta_a \left(\frac{\vartheta_{o\max}}{\vartheta_a} - \frac{\vartheta_{o\min}}{\vartheta_a} \right)$$

For 7 percent cooling air and $\vartheta_a = 804^\circ$ corresponding to 900° gas temperature one obtains the following temperature difference:

$$\Delta t_{max} = 140^\circ \text{ C}$$

Schörner 6 also measured temperature differences of more than 100° in the cross section of a hollow blade the interior of which was provided with ribs, to improve the cooling effect.

V. CALCULATION OF THE HEAT STRESSES

General Remarks on Thermal Stresses

Due to the temperature differences in the blade cross section, there appear thermal stresses. The effect of the thermal stresses can become so strong that heat cracks originate. The photograph (fig. 32) shows a series of blades H3 in which after a test run cracks were found on the convex[2] side. At first this phenomenon could not be explained satisfactorily. It could be proved by investigation of the temperature distribution and determination of the thermal stresses that the cracks are caused by the temperature differences in the cross section.

The thermal stress in a rod-shaped body the heat expansion of which is prevented by a fictitious rigid clamping of the ends according to figure 33, is [7]

$$\sigma = -E\beta\left(t - t_1\right)$$

t and t_1 are the temperatures distributed evenly over the cross section. The rod is heated from the temperature t_1 to the temperature t. E is the modulus of elasticity, β the linear heat expansion coefficient. When the heat expansion is completely prevented, very large stresses appear. For the austenitic steel SAS 8 E and β are for 600° C

$$\beta = 19 \times 10^{-6}\ 1/C^{\circ}$$

$$E \sim 1.5 \times 10^{6}\ kg/cm^2$$

For a heating of 10° one obtains a stress of

$$\sigma = 1.5 \times 10^{6} \times 19 \times 10^{-6} \times 10 = 285\ kg/cm^2$$

$$\sigma = 2.85\ kg/mm^2$$

---

[2]Literally: "belly side"

For temperature differences of about 100 one obtains thermal stresses in the order of magnitude of the elastic limit and the fatigue strength, respectively, of the heat resistant materials.

If the clamping is not completely rigid so that the rod can expand by the amount ϵ, the thermal stress becomes

$$\sigma = E\left[\epsilon - \beta\left(t - t_1\right)\right]$$

Calculation of the Thermal Stresses in a Rod Clamped on One Side with Arbitrary Temperature Distribution

A rod is considered which, like a turbine blade, is clamped at one end only; in this case the rod can expand freely and no thermal stresses appear as long as the temperature distribution in the cross section remains constant. If, however, the temperature distribution is not uniform, the separate fibers of the rod will interfere with each other. The cross section of the rod is, for instance, assumed rectangular according to figure 34 and the temperatures of the outer fibres t_1 and t_2. The upper fiber will expand more strongly than the lower one and the rod will bend.

Thus the stresses are partially reduced in comparison with the rigidly clamped rod which cannot bend.

In general, this problem can be represented as follows. Thin-walled bodies only will be discussed so that the stresses perpendicular to the wall can be neglected. For a rod-shaped body with a cross section according to figure 35, which is not subjected to external forces and is clamped on one end, the moment of the internal stresses must become zero in every section. Moreover, the sum of the internal stress itself must disappear. Thus, with the designations of figure 35, the following equations must be valid:

$$P = \int \sigma_z \, df = 0$$

$$M_x = \int \sigma_z y \, df = 0$$

$$M_y = \int \sigma_z x \, df = 0$$

The moment of the internal forces equals zero, if it is zero for any two axes.

Further, it is assumed, as in the theory of the bending of a rod that the cross sections remain plane. Under this assumption the statement (equation of a plane) can be made for the elastic deformations

$$\epsilon = \epsilon_o + \beta k_1 x + \beta k_2 y$$

One now considers the first condition $P = 0$. If one applies the formula given above for the stresses to an element of the rod, one obtains the following:

$$P = 0 = \int \sigma_z \, df = E \int \left[\epsilon - \beta\left(t - t_1\right)\right] df$$

If one now introduces the linear formulation for ϵ according to the equation above, it becomes

$$P = 0 = E \int \epsilon_o \, df + \int \beta k_1 x \, df + \int \beta k_2 y \, df - \beta \int \left(t - t_1\right) df$$

The integrals are transformed as follows:

$$\int \epsilon_o \, df = \epsilon_o f$$

The dilatation ϵ_o was assumed to be constant. The second integral represents the static moment of the cross section, referred to the y-axis, and can, according to the center-of-gravity theorem, be equated to fe_1e_1 is the distance of the center of gravity from the y-axis. The integral $\int y \, df$ also can be transformed

accordingly. Then $\int t\,df = tmf$ with t_m representing the mean temperature of the cross section. Thus one obtains

$$\int \epsilon_o\,df = \epsilon_o f$$

$$\int k_1 x\,df = k_1 e_1 f$$

$$\int k_2 y\,df = k_2 e_2 f$$

$$\int t\,df = tmf$$

$$\int t_1\,df = t_1 f$$

The temperature of reference t_1 contained in the formulas is equated to the mean temperature of the cross section. The expression then becomes

$$\beta \int (t - t_1)\,df = 0$$

The first condition $P = 0$ yields therefore the relation

$$\epsilon_o = k_1 e_1 + k_2 e_2 = 0$$

Then the condition $Mx = 0$ and $My = 0$ is considered. If the coordinate system is selected so that it goes through the center

of gravity, e_1 and e_2 equal zero. One may assume that the following derivations will be particularly simple if one selects a system of coordinates going through the center of gravity.

The condition $Mx = 0$ yields

$$M_x = 0 = E\left[\int \epsilon_o y \, df + \int \beta k_1 xy \, df + \int \beta k_2 y^2 \, df - \int \beta (t - t_m) y \, df\right]$$

One equates

$$\int xy \, df = I_{xy}$$

$$\int y^2 \, df = I_{xx}$$

$$\int ty \, df = I_{tx}$$

For an axis through the center of gravity the integral is $\int y \, df = 0$.

Thus one obtains:

$$0 = 0 + \beta k_1 I_{xy} + \beta k_2 I_{xx} - \beta I_{tx}$$

For the third condition $My = 0$ there results

$$M_y = 0 = E\left[\int \epsilon_o x \, df + \int k_1 x^2 \, df + \int k_2 xy \, df + \int \beta (t - t_m) x \, df\right]$$

One designates

$$\int x^2 \, df = I_{yy}$$

$$\int tx \, df = I_{ty}$$

and takes into consideration that $\int x \, df$ for the axes through the center of gravity equals zero. Then

$$0 = 0 + \beta K_1 I_{yy} + \beta K_2 I_{xy} - \beta I_{ty}$$

So far it was assumed that the coordinate system goes through the center of gravity of the profile. If the coordinate system is selected so that it coincides with the main axes of inertia, the integral also becomes

$$I_{xy} = \int xy \, df = 0$$

From the three conditions $P = 0$, $M_x = 0$, $M_y = 0$ one therefore obtains

$$\epsilon_o = 0$$

$$K_1 = \frac{I_{ty}}{I_{yy}}$$

$$K_2 = \frac{I_{tx}}{I_{xx}}$$

The thermal stresses are calculated as follows:

$$\sigma = E\left[\epsilon - \beta\left(t - t_m\right)\right]$$

$$\sigma = \beta E\left[K_1 x + K_{2y} - \left(t - t_m\right)\right]$$

The temperature distribution in the cross section is assumed given by the temperature field determined in the preceding section and represented by the isotherms. In the equation above $k_1 x$ represents a temperature and one may write

$$t_o = K_1 x + K_2 y + tm$$

This equation represents a temperature plane which can also be given by the isotherms. Thus the thermal stress becomes

$$\sigma = \beta E\left(t_o - t\right)$$

Temperature and Stress Field for the Hollow Blade H8

In the cross section of the blade H8 (fig. 36) two isotherm fields are superimposed. One now connects the points where the temperature difference of the two fields is equal, for instance, the point at which the isotherm of the temperature variation 700° intersects the isotherm of the auxiliary plane 700° with the point at which the isotherm of the temperature field $t = 650^\circ$ intersects the isotherm of the auxiliary plane $t_o = 650^\circ$, etc. The lines of equal temperature difference that were thus obtained represent simultaneously lines of equal thermal stresses. Figure 37 gives the stress field for the hollow blade H8 which was determined in this manner.

VI. CONSIDERATION OF THE EFFECT OF THE RADIATION ON THE BLADE TEMPERATURE

The Magnitude of the Heat Radiation

For high gas temperatures, the walls of the nozzles radiate so strongly that the heat transfer by radiation compared with the heat transfer by conduction must no longer be neglected. The heat quantity transferred by radiation between two walls is proportional to the fourth power of the temperatures according to the equation

$$Q = \text{Constant} \left(T_a^4 - T^4 \right)$$

At first it is assumed that the temperature of the radiating surface (nozzle blades) is T_a. If one refers the heat quantity transferred by radiation to the temperature difference of the radiating bodies, one obtains as the heat transfer coefficient by radiation

$$\alpha_s = c_s \frac{\left(\frac{T_a}{100}\right)^4 - \left(\frac{T}{100}\right)^4}{T_a - T} = c_s \left(T_a^3 + T_a^2 T + T_a T_o^2 + T_o^3 \right)$$

For oxidized surfaces for technical use, one has to insert in this formula for c_s: $c_s = 4.6$. In deriving the formula the number 100 in the denominator is omitted.

Derivation of a Relation for the Influence of the Radiation on the Mean Blade Temperature

In deriving the mean temperature of the cross section one introduces instead of α_a the value $\alpha_a + \alpha_s$ and obtains:

$$\left(\alpha_s + \alpha_a \right) U_a \left(T_a - T_{os} \right) = \alpha_1 U_1 \left(T_{os} - T \right)$$

From this equation there results

$$\frac{T_{os}}{T_a} = \frac{\alpha_a U_a \vartheta_a + \alpha_s \vartheta_a + \alpha_i U_i \vartheta_i}{\alpha_a U_a + \alpha_s U_a + \alpha_i U_i} = \frac{\alpha_a + \alpha_s + \frac{U_i}{U_a}\frac{\vartheta_i}{\vartheta_a}\alpha_i}{\alpha_a + \alpha_s + \frac{U_i}{U_a}\alpha_i}$$

With

$$\frac{U_i}{U_a} = m \qquad \frac{\vartheta_i}{\vartheta_a} = m$$

$\frac{T_{os}}{T_a}$ becomes

$$\frac{T_{os}}{T_a} = \frac{\alpha_a + \alpha_s + mn\alpha_i}{\alpha_a + \alpha_s + n\alpha_i} - \frac{\alpha_a + \alpha_s + n\alpha_i + n(m-1)\alpha_i}{\alpha_a + \alpha_s + n\alpha_i}$$

$$= 1 + \frac{n(m-1)\alpha_i}{\alpha_a + n\alpha_i + \alpha_s}$$

$$\frac{T_{os} - T_a}{T_a} = \frac{n(m-1)\alpha_i}{\alpha_a + n\alpha_i + c_s\left(T_{os}^3 + T_{os}^2 T_a + T_{os} T_a^2 + T_a^3\right)}$$

If one performs the multiplication, one obtains

$$T_a n(m-1)\alpha_i = T_{os}\left[\alpha_a + n\alpha_i + c_s(\cdots)\right] - T_a\left[\alpha_a + n\alpha_i + c_s(\cdots)\right]$$

Finally,

$$T_a n(m - 1)\alpha_i = \left(T_{os} - T_a\right)\left(\alpha_a + n\alpha_i\right) + c_s\left(T_{os}^4 - T_a^4\right)$$

From the relation for the mean blade temperature without radiation effect one obtains

$$T_a\left(\alpha_a + nm\alpha_i\right) = T_o\left(\alpha_a + n\alpha_i\right)$$

$$T_a\left(nm\alpha_i - n\alpha_i + \alpha_a + n\alpha_i\right) = T_o\left(\alpha_a + n\alpha_i\right)$$

$$T_a n(m - 1)\alpha_i = T_o - T_a\left(\alpha_a + n\alpha_i\right)$$

If one subtracts the equations from each other the result is

$$0 = \left(T_{os} - T_o\right)\left(\alpha_a + n\alpha_i\right) + c_s\left(T_{os}^4 - T_a^4\right)$$

If one designates the temperature difference between the mean temperature with and without radiation effect by ΔT, one obtains for it

$$\Delta T = \frac{c_s\left(T_a^4 - T_{os}^4\right)}{\alpha_a + n\alpha_i}$$

In this equation T_{os} is still unknown. One writes

$$T_{os} = T_o + \Delta t$$

Neglecting the higher powers, one obtains

$$T_{os}^4 = T_o^4 - 4T_o^3\,\Delta t$$

If this expression is introduced into the equation for ΔT, ΔT becomes finally

$$\Delta T = c_s \frac{\left(\frac{T_a}{100}\right)^4 - \left(\frac{T_o}{100}\right)^4}{\alpha_a + \frac{U_i}{U_a}\alpha_i + 0.04 c_s \left(\frac{T_o}{100}\right)^3}$$

With the temperature T_o without radiation effect given, the influence of the radiation Δt can be calculated by means of the formula above.

Complete Calculation of an Example

The blade H7 for 900° gas temperature according to the example in the second section is considered. For 8 percent cooling air quantity, ϑ_o/ϑ_a then is 0.71. For a stagnation temperature of 840° C ϑ_o becomes 573° C. With $\alpha_a = 258$, one obtains for the temperature rise at a location of the blade subject to radiation

$$\Delta t = 75^\circ$$

Thus one can see that occasionally essential increases in temperature may occur due to radiation of the hot nozzles. It was presumed for the preceding derivation that the nozzle wall takes on the stagnation temperature ϑ_a. It is known, however, that the walls of nozzles do not have the temperature of the flowing gas but about the temperature of the gas ahead of the nozzles. That would mean for this case that the nozzle walls take on the gas temperature, that is, for instance 900°, compared with a stagnation temperature of 804°. The maximum difference between gas temperature and stagnation temperature, however, appear only for the running turbine for which the flow velocity relative to the blade has the smaller value of $w_1 = c_1 - u_1$ instead of the nozzle exit velocity c_1. For segment tests, $w_1 = c_1$. Then the stagnation approximately equals the gas temperature. In figure 38 the mean temperature ϑ_o

for the hollow blade H7 is represented as a function of the cooling-air quantity with and without radiation effect.

Influence of the Radiation on the Nozzle Temperature

Thus the preceding derivation for the increase of the blade temperature ϑ_o by radiation, with the temperature of the nozzle walls equated to ϑ_o, is valid exactly only for the evaluation of segment tests. The fact is neglected that the nozzle walls themselves experience a temperature drop due to the heat radiations to the turbine blade. The following derivation will take into account that the actual temperature of the nozzle wall lies between gas and stagnation temperature. For the temperature of the nozzle wall the relation

$$2\alpha_{a_{nozzle}}\left(T_{gas} - T_{nozzle}\right) = c_s\left[\left(\frac{T_{nozzle}}{100}\right)^4 - \left(\frac{T_{os}}{100}\right)^4\right]$$

is valid if one takes into consideration that heat is transferred to the nozzle wall by convection on both sides whereas heat is radiated only on one side. One equates

$$T_{gas} - T_{nozzle} = \Delta t_{nozzle}$$

Then there is

$$\Delta t_{nozzle} = \frac{c_s\left[\left(\frac{T_{nozzle}}{100}\right)^4 - \left(\frac{T_{os}}{100}\right)^4\right]}{2\alpha_{a_{nozzle}}}$$

In this formula T_D and T_{os} are at first unknown. In calculating Δt_{nozzle} one may choose the procedure to calculate first an approximate value of $\Delta t_{nozzle} = \Delta t'_{nozzle}$ for various T_{os},

by equating $T_D = T_{gas}$. Then one calculates a first approximation for

$$T'_{nozzle} = T_{gas} - \Delta t_{nozzle}$$

With this value one obtains a second approximation of Δt_{nozzle}. Thus the solution of the equation of the fourth order can be avoided. In figure 39 the drop of the nozzle temperature is plotted for 900° gas temperature and a heat transfer coefficient $\alpha_{a_{nozzle}} = 300$. With these values the nozzle temperature becomes somewhat larger than the stagnation temperature. However, for the evaluation of the segment tests one may calculate with $T_{nozzle} = T_a$.

VII. TESTS ON BLADE SEGMENTS AND COMPARISON WITH THE CALCULATION

Description of the Tests

These tests were performed on a blade segment on the scale 1:1 with 7 blades H3 (table II). The blades were heated by gas from a combustion chamber. The cooling air and combustion air were supplied by two rotary piston compressors. In the following discussion only the test points 7 and 8 at the center of the blade and 17 and 18 at the blade edges (fig. 40) are considered out of about 25 test points distributed over different blades. These test points are in the neighborhood of the blade tips so that the heat conduction to the rotor disc is negligible. The ratios of the measured temperatures and the gas temperatures are set up and plotted as functions of the cooling-air quantity. The test results for 700°and 900° gas temperature and the velocities w_1 between 200 and 350 meters per second were used.

Result of the Tests

The assumptions made for calculating the temperature $\vartheta_{o_{min}}$ are valid for the test points 7 and 8. In figure 41 the measured temperatures for test points 7 and 8 are plotted together with the calculated temperature $\vartheta_{o_{min}}$ for comparison. The calculated temperatures are slightly higher than the measured ones. The thermowires were led to the outside through the cooling ducts. The

cooled wire removes heat from the blade wall so that the presence of the measuring wire at the test point causes a drop in temperature. In the next section the error of measurement caused by the installation of the thermowires in the gas or cooling air flow will be further investigated.

The test points 17 and 18 are close to the blade edges. The temperature can be determined according to the indications in section IV. Figure 42 contains the measured temperatures for the test points 17 and 18 and, for comparison, the temperature calculated for test point 17. Here also the calculated values are higher than the test values although these test points were installed in grooves, so that the error due to the thermowires was eliminated. Moreover, an additional heating should occur at the test point 17 due to radiation of the nozzles.

The differences between the temperatures of the blade edges, test points 17 and 18, and the temperatures of the blade center, test points 7 and 8, are correctly represented by the calculation. The agreement of measured and calculated values with respect to magnitude also is very good since the latter values are on the average only 2 to 3 percent higher than the former ones.

VIII. ERROR OF MEASUREMENT FOR THE INSTALLATION OF THERMOWIRES IN THE AIR AND GAS FLOW, RESPECTIVELY

Origin of the Error

For temperature measurements on gas-turbine blades, great difficulties often arise in the installation of the thermocouples. For small wall thicknesses below 1 millimeter, in particular, a reliable installation in grooves or bore holes is no longer possible. The thermowires toward the outside have to be freely guided in the gas or air flow. The conductivity of the thermowire causes here an error. On the cooling air side of the blade wall the measuring wire is located in the cold cooling air flow and removes heat from the blade wall so that a temperature drop appears at the test point. On the gas side the wire becomes warmer than the blade wall and additional heat flows into the wall causing a rise in the wall temperature at the test point. The magnitude of the error due to the presence of the wire will now be determined.

Derivation of a Formula for the Magnitude of the Error

A part of the blade wall of the thickness δ is considered, with a thin wire of the thickness $2r_1$ running into it. In the

blade wall the heat flows radially toward the measuring wire. An annular cut-out of the radius r and the thickness dr is considered. The heat content Q_3 enters this annular element of the blade wall from the gas side according to the following relation:

$$Q_3 = \alpha_a 2\pi r \, dr\left(\vartheta_a - \vartheta\right)$$

ϑ being the wall temperature at the distance r from the center of the wire. On the cooling air side of the blade wall, the heat content Q_4 is absorbed by the cooling air flow.

$$Q_4 = \alpha_i 2\pi \, dr\left(\vartheta - \vartheta_i\right)$$

Here again the temperature differences at tight angles to the blade wall have been neglected. For the heat flow in the blade wall the relation is valid

$$Q_1 - Q_2 = \lambda_w 2\pi \vartheta \left(r \frac{d^2\vartheta}{dr^2} + \frac{d\vartheta}{dr}\right) dr$$

The heat content entering the annular element is assumed to be positive, the heat content leaving it, negative. Then the equation is valid:

$$Q_1 - Q_2 + Q_3 - Q_4 = 0$$

Therefrom one obtains the differential equation

$$\frac{d^2\vartheta}{dr^2} + \frac{1}{r}\frac{d\vartheta}{dr} + \frac{\alpha_a}{\lambda_w \vartheta}\left(\vartheta_a - \vartheta\right) - \frac{\alpha_i}{\lambda_w \vartheta}\left(\vartheta - \vartheta_i\right) = 0$$

Therefrom one obtains the differential equation

$$\frac{\alpha_a}{\lambda_w \vartheta} + \frac{\alpha_1}{\lambda_w \vartheta} = a$$

and

$$\frac{\alpha}{\lambda_w \vartheta} \vartheta_a + \frac{\alpha_1}{\lambda_w \vartheta} \vartheta_1 = a \vartheta_2$$

one obtains the following Bessel's differential equation of zero order

$$\frac{d^2 \vartheta}{dr^2} + \frac{1}{r} \frac{d \vartheta}{dr} + a\left(\vartheta_2 - \vartheta\right) = 0$$

or, with $-\theta = \vartheta_2 - \vartheta$ there results

$$\theta'' + \frac{1}{r}\theta' - a\theta = 0$$

The solution reads:

$$\theta = AI_o\left(i\sqrt{a}r\right) + B_i H_o\left(i\sqrt{a}r\right)$$

At great distance from the wire, that is, for $r = \infty$, $\theta = 0$ or $\vartheta = \vartheta_2$. Upon insertion of these values one obtains

$$\theta_2 = AI_o(\infty) + B_i H_o(\infty)$$

One obtains $A = 0$, because of $I_o(\infty) = \infty$. Thus there remains

$$\theta = B_1 H_o\left(i\sqrt{a}r\right)$$

The constant B is determined from the magnitude of the heat content flowing in and flowing away through the wire. One considers the wire as a rod of the circumference $U = 2\pi r_1$, and the cross section $f = r_1^2\pi$; then the resulting heat content flowing through the rod [8] is

$$Q = \frac{\alpha_{Dr} U}{\beta}\left(\vartheta_1 - \vartheta_i\right)\tan(\beta h)$$

Since the wire must be regarded as long in relation to the diameter, one may equate $\tan(\beta h) = 1$. ϑ_1 is the temperature at the point $x = 0$, that is, at the wall. At large distance from the wall the wire assumes the temperature of the cooling air, designated by ϑ_i. The heat content Q leaving through the wire must enter the wire from the wall. If one considers a cylinder of the radius r_1 in the blade wall, the relation

$$Q = \lambda 2\pi r_1 \vartheta\left(\frac{d\theta}{dr}\right)$$

is valid for the heat flow. From this relation one determines $\left(\frac{d\theta}{dr}\right)_1$; from this value the missing constant B then results as follows:

$$\left(\frac{d\theta}{dr}\right)_1 = B\sqrt{a}iH_1\left(i\sqrt{a}r_1\right)$$

The constant B becomes

$$B = \frac{\frac{\alpha_{Dr} U}{\beta}\left(\vartheta_1 - \vartheta_i\right)}{\lambda_w 2\pi r_1 \vartheta \sqrt{a}\, iH_1\left(i\sqrt{a} r_1\right)}$$

For determination of this constant the assumption was made that the heat flow in the wall will be radial up to a radius r_1. Actually the heat flow lines will deviate before that. Thus the calculation was carried out under simplified, not wholly exact assumptions. The error θ_1, that is, the difference between the wall temperature without wire ϑ_2 and the temperature at the location of the wire ϑ_1 is determined as follows. The constant was

$$B = \frac{\theta_1}{iH_o\left(i\sqrt{a} r\right)} = \frac{\frac{\alpha_{Dr} U}{\beta}\left(\vartheta_1 - \vartheta_i\right)}{\lambda_w 2\pi r_1 \vartheta \sqrt{a}\, iH_1\left(i\sqrt{a} r_1\right)}$$

One equates the expression

$$\frac{\alpha_{Dr} r_1 \lambda_{Dr}}{2\alpha \vartheta \lambda_w} \frac{iH_o\left(i\sqrt{a} r_1\right)}{iH_1\left(i\sqrt{a} r_1\right)} = XY$$

Then θ is

$$\theta_1 = \vartheta_2 - \vartheta_1 = XY\left(\vartheta_1 - \vartheta_i\right)$$

further,

$$\vartheta_1 = \vartheta_2 - \theta_1$$

and therefore

$$\theta_1 = XY\left(\vartheta_2 - \theta_1 - \vartheta_i\right)$$

One obtains

$$\theta_1 = \frac{XY\left(\vartheta_2 - \vartheta_i\right)}{1 + XY}$$

or, written in a different form,

$$\frac{\theta_1}{\vartheta_2 - \vartheta_i} = \frac{1}{1 + XY}$$

The left side represents the error referred to the difference between wall temperature and cooling-air temperature. One may represent the error as a function of the two values

$$X = \frac{H_1\left(i\sqrt{a}r_1\right)}{H_o\left(i\sqrt{a}r_1\right)}$$

$$Y = \sqrt{\frac{2\alpha^2\lambda_w}{\alpha_{Dr}r_1\lambda_{Dr}}}$$

in percent of the temperature difference $\vartheta_2 - \vartheta_1$. In order to simplify the manipulation, the error is represented if figure 44 as a function of the values

$$x = \sqrt{\frac{\alpha r_1^2}{\lambda_w \delta}}$$

$$y = \sqrt{\frac{2\alpha\delta\lambda_w}{\alpha_{Dr} r_1 \lambda_{Dr}}}$$

Complete Calculation of an Example

The use of the chart (fig. 44) will be discussed on hand of an example. The following values are given.

Temperature of the blade wall without thermocouple, ϑ_2, °C	600
Cooling-air temperature, ϑ_1, °C	150
Heat transfer coefficient on the gas side, α_a, K cal/m², °C, h	258
Heat transfer coefficient on the cooling air side, α_i, K cal/m², °C, h	155
Heat transfer coefficient on the thermowire, α_{Dr}, K cal/m², °C, h	1180
Heat conductivity of wire and blade wall, λ, K cal/m, °C, h	18
Wall thickness, δ, mm	1
Wire thickness, $2r_1$, mm	0.5

One now determines the two characteristic values

$$x = \sqrt{\frac{(\alpha_i + \alpha_a) r_1^2}{\lambda_w \delta}} = \sqrt{\frac{413 \times 0.25^2 \times 1000}{18 \times 1000^2 \times 1.0}} = 0.0379$$

$$y = \sqrt{\frac{2\alpha\delta}{\alpha_{Dr} r_1}} = \sqrt{\frac{2 \times 413 \times 1}{1180 \times 0.25}} = 1.67$$

Figure 44 gives the error of measurement for these values as 7 percent. The error itself is

$$\theta_1 = 0.07\left(\vartheta_2 - \vartheta_1\right) = 0.07 \times 450 = 31.5^\circ \text{ C}$$

Thus the error can be determined in a simple manner with the aid of the characteristic values x and y.

IX. POWER REQUIREMENT FOR COOLING AND PROSPECTS OF THE HOLLOW-BLADE TURBINE

Power Required for Cooling the Turbine Rotor

The turbine rotor with the hollow blades has the effect of a centrifugal compressor. The cooling air leaving the turbine rotor has the circumferential component $cu_2 = u_a$. Thus the work absorbed by 1 kilogram cooling air is

$$H_{total} = \frac{1}{c}\left(u_a cu_2\right) = \frac{u_a^2}{g} \text{ mkg/kg}$$

The power absorbed by the cooling air then is

$$N_{cool} = \frac{G_K H_{total}}{75} \text{ ps}$$

The turbine power is

$$N_T = \frac{G_{gas} H_o \eta_T}{75}$$

The turbine gradient H_o can be expressed by the ratio u/c_o as follows:

$$H_o = \frac{c_o^2}{2g} = \left(\frac{c_o}{u}\right)^2 \frac{u^2}{2g}$$

it is customary to insert the mean circumferential velocity of the turbine rotor. The relation between mean circumferential velocity and maximum circumferential velocity u_a is:

$$\frac{U_a}{U} = \frac{D_a}{D_m} = \left(1 + \frac{l}{D_m}\right)$$

with l designating the length of the turbine blade. One now forms the ratio cooling power requirement/turbine power:

$$\frac{N_{cool.}}{N_T} = \frac{G_K}{G_{gas}} \frac{H_{total}}{H_o \eta_T} = \frac{2u_a^2/2g}{(c_o/u)^2 \frac{u^2}{2g} \eta_T} p$$

$$n = \frac{N_{cool.}}{N_T} = \frac{2}{(c_o/u)^2} \left(1 + \frac{l}{D_m}\right)^2 \frac{1}{\eta_T} p$$

For the examples mentioned, H5 and H7, the ratio is $l/D_m = 0.166$. The optimum efficiency of a turbine is obtained for a certain ratio u/c_o, a value lying between 0.4 and 0.5. If one assumes, moreover, an efficiency, for instance $\eta_T = 0.75$, all values in the equation above are known and the power ratio is proportional only to the percent cooling air mass. n becomes:

$$n = 2\left(\frac{u}{c_o}\right)^2 \left(1 + \frac{l}{D_m}\right)^2 \frac{1}{\eta_T} p$$

$$n = 2(0.4 \div 0.5)^2(1 + 0.166)^2 \frac{1}{0.75} p = (0.58 \div 0.91)p$$

The power requirement for cooling is therefore independent of the magnitude of the circumferential velocity.

Feeding Performance of the Blade Star

The static work head of the turbine rotor may be calculated as follows. One assumes that the circumferential component of the cooling-air velocity at every point is $c_u = u = r\omega$, that is, that the flow goes through radial ducts. Then the static pressure increase on the way from $r = 0$ to r is

$$\int_o^r \frac{dp}{\gamma} = \int_o^r \frac{1}{g} \frac{c_u^2}{r} dr = \int \frac{1}{g} \frac{\omega^2 r^2}{r} dr = \frac{\omega^2}{g} \left| \frac{r^2}{2} \right|_o^r$$

$$= \frac{u^2}{2g} = H_{stat}$$

In a turbine rotor of a mean circumferential velocity of 300 meters per second, the circumferential velocity at the blade tip corresponding to $D_a/D_m = 1.166$ is $U_a = 350$ meters per second. The static work head becomes

$$H_{stat} = \frac{u^2}{2g} = 6250 \text{ mkg/kg}$$

A pressure ratio of about 1.8 corresponds to this work head. Flow tests for various hollow blades are reproduced in figure 45. A pressure ratio of about 1.35 is required for a cooling air quantity of 7.5 percent. The actually present pressure ratio is 1.8. The feeding performance of the turbine rotor is therefore sufficient to press the cooling air through the blade ducts and, moreover, to feed the cooling air against a certain excess pressure toward the turbine rotor. For a favorable design of the blade shape, sufficient cooling can be obtained with 5 percent cooling air for 300 meters per second circumferential velocity and 900° gas temperature. The power requirement for cooling then is 2.9 to 4.5 of the turbine power.

Power and Efficiency of a Gas-Turbine Apparatus for a Temperature Increase to 850°

The improvement of the thermic efficiency of the turbine arrangement by higher temperatures corresponds to this cooling requirement. A gas turbine installation with uncooled blades and a hollow blade turbine shall be considered for comparison. The operating temperatures of the fuel gas ahead of the turbine are assumed to be 550° or 850° C. In table VIII both arrangements are compared. A larger compression ratio is useful for higher gas temperature. The values for the internally cooled turbine are taken from a publication about tests on a turbine apparatus manufactured by BBC [9].

As shown in table VIII, one obtains by increase of the temperature to 850° ahead of turbine with the same blower an increase of the useful power from 5700 to 12000 PS (German HP), that is, to about twice the amount. For equal design requirements the useful power becomes, therefore, essentially larger. In other words, the air requirement per PS useful power which is decisive for the size of the engine will be about half as large. The thermic efficiency increases from 18 to 20.1 percent if one inserts 5 percent of the turbine power as the power required for cooling.

For the BBC apparatus the temperature behind the blower is 203°. The temperature of the exhaust gases is given as 278°. Thus the temperature difference between air and exhaust gas which is decisive for the utilization of the exhaust heat is only 75°. A heat exchanger will, therefore, not be of great use in this case and was, for that reason, omitted in the BBC - installation. The conditions in the apparatus with 850° gas temperature are different. There the resulting temperature behind the turbine is 556°. The temperature difference between gas and air is here much larger and

amounts to $556^\circ - 203^\circ = 353^\circ$. The following expression is designated as factor of merit of the heat exchanger:

$$\eta_{cool.} = \frac{t2_{air} - t1_{air}}{t1_{gas} - t1_{air}} = \frac{\Delta t_{air}}{t1_{gas} - t1_{air}}$$

A factor of merit of 0.4 - 0.45 can be reached without a particularly large expenditure. For a factor of merit $\eta_{cool.} = 0.4$ one obtains for the 850° - apparatus the following values (table IV), if the blower remains unchanged.

The combustion air is preheated to 344° C in the heat exchanger, thus reducing the fuel quantity from 3740 kg/h to 2950 kg. Correspondingly, the thermic efficiency of the apparatus rises from 20 to 25.4 percent and the specific fuel consumption decreases to 246 gr/PS_h.

For these considerations the compression ratio was taken over unchanged from the 550° - apparatus. It is known from various computational investigations that the most favorable compression ratio is higher for higher temperature ahead of turbine. Therefore, another example with a higher pressure behind blower of 6 ata shall be fully calculated. The blower efficiency is assumed somewhat smaller, as 84 percent, the turbine efficiency as before.

In table 10 the numerical values for the larger pressure ratio are compiled. The useful power increases by 1100 PS to 13100. The fuel consumption decreases because the compressed air leaves the blower at higher temperature. The thermic efficiency improves; it increases from 20 to 23.7 percent. The same apparatus with heat exchanger, again under assumption of a factor of merit of 0.4, has a thermic efficiency of 28.6 percent and a specific fuel requirement of 217 gr/PS h (table XI). These numerical values prove that with the hollow-blade turbine for temperatures of 800° to 900° an essential increase of fuel utilization and of useful power per kilograms per second combustion air is obtainable. The values given represent by no means the upper limit that could be reached.

Influence of the Exit Loss on the Turbine Efficiency

For the examples in the first section the circumferential velocities considered were 250 and 300 meters per second. Now the

problem remains to be investigated whether large circumferential velocities are useful also for gas-turbine apparatus where every percent efficiency matters. For large circumferential velocity, at first the same stage efficiency can be obtained as for small circumferential velocity as long as one remains below sonic velocity and avoids short blades with considerable slot loss. The use of large circumferential velocities results in a turbine with few stages only. The exit energy from the last stage is here very noticeable and deteriorates the total efficiency. If one considers a turbine stage with the velocity triangle according to figure 46, the exit energy is

$$h_A = \frac{c_2^2}{2g}$$

For the optimum efficiency, that is, perpendicular exit one obtains

$$\tan \alpha_2 = \frac{c_m^2}{u}$$

Therewith the exit energy becomes

$$h_A = \frac{c_{m2}^2}{2g} = \frac{u^2}{2g} \left(\tan \alpha_2\right)^2$$

The gradient utilized in the turbine stage is

$$H_o = c_o^2/2g$$

If one sets up a ratio exit energy/stage gradient, one obtains

$$\frac{h_A}{H_o} = \left(\frac{u}{c_o}\right)^2 \left(\tan \alpha_2\right)^2$$

For instance for an exit angle $\alpha_2 = 35^\circ$ and a characteristic value $u/c_o = 0.5$ the exit loss will be

$$\frac{h_A}{\Sigma H_o} = 0.5^2 \times 0.7^2 = 0.123 = 12.3 \text{ percent}$$

The exit loss may be reduced by smaller exit angles. For an exit angle of 25° smaller exit losses result, namely 5.4 percent for $u/c_o = 0.5$. The loss of exit energy can also be reduced by an exit diffuser, similar as for a water turbine where the exit energy, particularly for specific high-speed turbines, is of decisive influence on the efficiency. If there is a greater number of turbine stages, the exit energy is of less importance for the total efficiency.

For the gas-turbine apparatus represented in table 10 a preliminary design of a turbine of 300 meters per second circumferential velocity shall be made. One obtains a three-stage turbine, with only the two first stages cooled. The gradients and the corresponding temperatures are compiled in table XII.

The pertaining I-S diagram is shown in figure 47. The exit loss from the last stage is assumed as 12 percent. The exit loss then is, referred to the total gradient,

$$\frac{h_A}{H_o} = 12 \frac{35}{113} = 3.7 \text{ percent}$$

One can see that the influence of the exit energy can be kept small also for a small number of stages. For reason of simplicity of construction it is useful to select for high temperatures gas turbines with only a few high-speed stages.

Translated by Mary L. Mahler
National Advisory Committee
for Aeronautics

X. REFERENCES

1. Leist, K.: Der Laderantrieb durch Abgasturbinen. Jahrbuch d. Dt. Luftfahrtforschung 1937 p. II 137.

2. Knörnschild, E.: Die Ermittlung der Schaufeltemperatur von Gasturbinen. Jahrb. d. Dt. Luftfahrtforschg. 1940 II p. 291.

3. Eckert, E., and Weise: Die Temperatur ungekühlter Turbinenschaufeln in einem schnellen Gasstrom. Dt. Luftfahrtforschg. FB 1387 (ZWB).

4. Lutz: Wandtemperatur beim Wärmedurchgang durch Wände von beliebiger Form. VDI-Zeitschrift 1935 p. 1041.

5. Schmidt and Wenner: Messung der Verteilung der Wärmeabgabe über den Umfang eines senkrecht zur Achse angeblasenen geheizten Zylinders. Jahrb. d. Dt. Luftfahrtforschg. 1940 p. II 135.

6. Schörner: Untersuchungen über die Beherrschung hoher Gastemperaturen bei Abgasturboaufladung durch Innenkühlung. Jahrb. d. Dt. Luftfahrtforschg. 1938 p. II 219.

7. ten Bosch: Vorlesung über Maschinenelemente. 2. Auflage 1940, Abschn. 12.6 p. 64.

8. ten Bosch: Die Wärmeübertragung. 3. Auflage 1936 p. 59.

9. Stodola: Leistungsversuche an einer Verbrennungsturbine. VDI-Zeitschrift 1940 p. 17.

TABLE I

Temperature ahead of nozzle, °C	900	900
Circumferential velocity u, m/sec	250	300
Nozzle angle α_1	24°30'	24°30'
Angle of flow incidence of the blade β_1, deg	41	41
Nozzle exit velocity, m/sec	575	692.5
Relative velocity of the flow with respect to the blade, m/sec	365	435
Nozzle contraction coefficient ϵ	0.85	0.85
Cooling-air temperature ϑ_1, C	150	150
Stagnation temperature ϑ_a, C	805	762

TABLE II

Blade	H3	H5	H7	H8
Mean diameter D_m	277	283	283	527.5
Blade { length	46	47	47	87.7
Blade { width	16	19	18	26
Blade { number	80	60	66	90
Blade { spacing	10.89	14.81	12.35	18.4
Mean cooling duct { area	24.37	32.1	28.5	59.9
Mean cooling duct { circumference	21.8	30.0	47.5	35.7
External circumference U_a	41.88	50	50.5	69.6
Mean blade cross section	37.23	48.6	43.0	102.1
Nozzle { height	39	41	41	./.
Nozzle { angle	20	24°30	24°30'	
U_i/U_a	0.521	0.60	0.937	0.513
F_i/hts	0.0574	0.0527	0.0563	./.
$d_a = U_a/\pi$	13.3	15.9	16.07	22.2
$d_i = \frac{4f_k}{U_i}$	4.46	5.27	2.615	6.7

Linear dimensions in mm, areas in mm^2.

TABLE III

Blade	H5	H7
$\left(\frac{F_{\sin}^{\beta}}{F_K}\right)^{0.735}$	5.636	5.4
$\left(d_a/d_i\right)^{0.265}$	1.416	1.614
$\left(T_i/T_a\right)^{0.183}$	0.843	0.843
$\left(\alpha_i/\alpha_a\right)$	3.465 p^m	3.78 p^m

TABLE IV

Blade	H5		H7	
Cooling air mass in percent	5	7.5	5	7.5
Re_a	13,600	13,600	13,720	13,720
Nu_a	72	72	72	72
α_a	226	226	258	258
β	125.7	130.0	156	164

TABLE V

Nozzle angle 40°35' Test of Oct. 6, 1941			Barometric pressure 728 mm Hg temperature 17.5° C	
Boiler pressure p_{boiler} (mm WS)	Static pressure in the nozzle p_{nozzle} (mm WS)	Pressure difference Δp (mm WS)	Specific weight γ (kg/m^3)	Velocity w_1 (m/sec)
28.5	13	15	1.167	16.15
43	20	23	1.169	19.65
66	29	37	1.171	24.9
95	40	55	1.174	30.4
113.5	47	66.5	1.178	33.3
165	69	96	1.183	39.92

TABLE VI

Nozzle angle 40°35' - Date: Sept. 23/24, 1941 - Barometric pressure 726 mm Hg

Test point no.	Boiler temperature (°C)	Boiler pressure (mm WS)	Intensity of current (Amp)	Voltage (volt)	Heat produced by current (k cal/sec)	Mean temperature of the blade ϑ_m (°C)	Temperature difference $\Delta\vartheta$ (°C)	Heat transfer coefficient α	Nusselt number Nu	Velocity w_1 (m/s)	Reynolds number Re
1	25	41	3.33	117.5	0.0934	66	41	99.7	394	19.15	103,300
2	25.7	41	3.98	142	.1347	85.6	59.9	98.4	388.5	19.15	103,000
3	26.3	40	4.53	164	.1774	103.9	77.6	99.8	394	18.9	101,300
4	26.2	40	5.0	185	.2208	124.1	97.9	98.75	390	18.9	101,300
5	26.2	64	3.44	122	.1001	65.2	39	112.3	443	24.4	130,800
6	26.2	64	4.28	155	.1584	86.3	60.1	115.8	457	24.4	130,800
7	25.6	64	4.85	180	.2083	104.5	78.9	115.5	456	24.4	131,100
8	25.5	64	5.4	202	.2602	124.4	98.9	115.2	454	24.4	131,100
9	13.6	105	4.28	155	.1584	66.1	52.5	132.8	542	31.9	183,100
10	13.6	105	4.9	183	.214	85.3	71.7	131.3	536	31.9	183,100
11	14.0	105	5.6	209	.2791	104.1	90.1	136.2	555	31.9	182,700
12	23.4	127	4.03	146	.1404	65.5	42.1	147	584	35.4	192,700
13	23.4	127	4.81	179	.2054	85.1	61.7	146.6	580	35.4	192,700
14	23.4	127	5.55	206	.2728	103.7	80.3	149.4	593	35.4	192,700
15	24.2	154	4.13	151	.1489	66	41.8	156.7	620	39	211,100
16	24.8	155	4.95	185	.2185	85.6	60.8	157.9	626	39.15	211,150
17	24.7	154	5.73	212	.2898	103.6	78.9	161.7	639	39	210,500

TABLE VII

Nozzle angle 40°35' - Date: Sept. 23/24, 1941 - Barometric pressure 726 mm Hg

Test point no.	Blade temperatures test point 1 ÷ 20 in, °C																			
	1	2	3	4	5	6	7	8	9	10	11	12	13	14	15	16	17	18	19	20
1	62	65	66.5	66.5	66	64	62	64.5	67.5	66	65	66.5	69	69	68.5	66	64	66	69	67
2	81	85	87	87	87	84	81	84.5	87	85	83	86	89	89	88.5	85	82	85	88.5	87
3	98	103	106	106	105.5	102	98	103	106	103.5	101	104	108.5	108	107.5	103	100	103	108	105
4	118.5	124	128	128	127	122	117	123	127	123.5	120.5	124	129	129	128	122.5	117	122.5	127.5	124.5
5	62	65	66.5	67	66.5	64.5	62	64.5	66.5	64.5	63.5	65	67	68	67	65	62.5	64.5	67	66
6	81	85	88	88	88	84.5	80.5	85	88	85	84	86	90	90	90	86	82.5	86	90	88
7	97	102.5	106	106	106	107	96.5	102.5	106.5	103.5	102	105	110.5	110	109	104	99	104	110	106.5
8	116	123	127	127	127	121	115	122.5	128	123	121	124.5	131	131	130	124	118	123	130	126
9	61	65	68	68	68	64	59.5	65	68	65.5	64	67	70.5	70.5	70	65.5	61	65	70	67
10	78.5	84.5	88.5	88.5	87.5	82.5	76.5	83	88	84.5	82	86	91	91	90	84	78.5	84	90	87
11	95	103	108	108	107	101	93	102.5	108	104	100.5	105	112	112	110.5	103.5	86	104	111	107
12	61	65	67	67.5	67	64	60	64	67.5	65.5	63.5	66	69	69	68.5	65	61	65	69	67
13	79	84.5	88	88	87.5	82.5	77	84	88	85	82	85	90.5	90.5	89	84	78.5	84	89.5	86.5
14	95	103	107	107.5	107	100	93	101.5	107.5	103	99.5	104	111	110.5	109	102.5	95	102.5	110	106
15	62	65.5	68	68	68	64	60	65	68	66	64	66	70	69.5	69	65	61	65	69	67
16	79	84.5	88	88.5	88	83	76.5	84	88.5	85.5	82	86	91	91	90	84.5	79	84.5	90.5	82
17	95.5	103	107.5	108	107	100	93	101.5	108	103.5	99	103	110.5	110.5	109.5	102	94.5	101.5	109	105.5

TABLE VIII

	BBC combustion turbine apparatus	Hollow-blade turbine apparatus
Blower:		
Temperature ahead of blower, °C	23	23
Temperature behind blower, °C	203	203
Pressure ahead of blower, kg/cm^2	0.988	0.988
Pressure behind blower, kg/cm^2	4.34	4.34
Air weight, t/h	222.8	222.8
Adiabatic gradient, K cal/kg	37.5	37.5
Adiabatic power, PS	13,200	13,200
Thermodynamic efficiency, percent	84.6	84.6
Power of the generator, PS	15,600	15,600
Turbine:		
Temperature ahead of turbine, °C	552	850
Temperature behind turbine, °C	278	566
Pressure ahead of turbine, kg/cm^2	4.27	4.27
Pressure behind turbine, kg/cm^2	1.00	1.00
Gas weight, t/h	224.8	226.4
Adiabatic gradient, K cal/kg	67.9	92.6
Adiabatic power, PS	24,100	33,200
Thermodynamic efficiency, percent	88.4	83.4
Power of the generator, PS	21,300	27,600
Combustion chamber:		
Heat value	10,140	10,140
Fuel quantity, kg/h	1,967	3,740
Power of the generator, PS	5,700	12,000
Thermic efficiency, percent	18	20.1
Specific fuel consumption, gr/PS h	346	311

TABLE IX

Heat exchanger:	
Factor of merit	0.4
Air temperature ahead of heat exchanger, °C	203
Air temperature behind heat exchanger, °C	344
Gas temperature ahead of heat exchanger, °C	566
Gas temperature behind heat exchanger, °C	436
Heating of the air, °C	141
Air quantity, t/h	222.8
Fuel quantity, kg/h	2950
Useful power, PS	12,000
Thermic efficiency, percent	25.4
Fuel consumption, gr/PS h	246

TABLE X

Blower:	
Temperature ahead of blower, °C	23
Temperature behind blower, °C	256
Pressure ahead of blower, ata	0.988
Pressure behind blower, ata	6.0
Air weight, t/h	222.8
Adiabatic gradient, K cal/kg	47.5
Adiabatic power, PS	16,800
Thermodynamic efficiency, percent	84.0
Power of the generator, PS	20,000
Turbine:	
Temperature ahead of turbine, °C	850
Temperature behind turbine, °C	509
Pressure ahead of turbine, kg/cm^2	5.90
Pressure behind turbine, kg/cm^2	1.000
Gas weight, t/h	226.2
Adiabatic gradient, K cal/kg	111
Adiabatic power, PS	39,700
Thermodynamic efficiency, percent	83.4
Power of the generator, PS	33,100
Heating value, K cal/kg	10,140
Fuel quantity, kg/h	3450
Power of the generator (useful power), PS	13,100
Thermic efficiency, percent	23.7
Specific fuel consumption, gr/PS h	263
Useful power per kg/sec combustion air, PS/kg	212

TABLE XI

Heat exchanger:	
Factor of merit	0.4
Temperature of air ahead of heat exchanger, °C	256
Temperature of air behind heat exchanger, °C	363
Temperature of gas ahead of heat exchanger, °C	509
Temperature of gas behind heat exchanger	
Heating of the air, °C	107
Air quantity, t/h	222.8
Fuel quantity, kg/h	2850
Useful power, PS	13,100
Thermic efficiency, percent	28.6
Specific fuel consumption, gr/PS h	217

TABLE XII

Stage	1	2	3
Gradient, K cal/kg	45	33	35
Temperature of gas ahead of stage, °C	850	704	596
Stagnation temperature, °C	747	631	542
Cooling air mass, percent	5	1.5	---
Blade temperature, °C	580	580	542

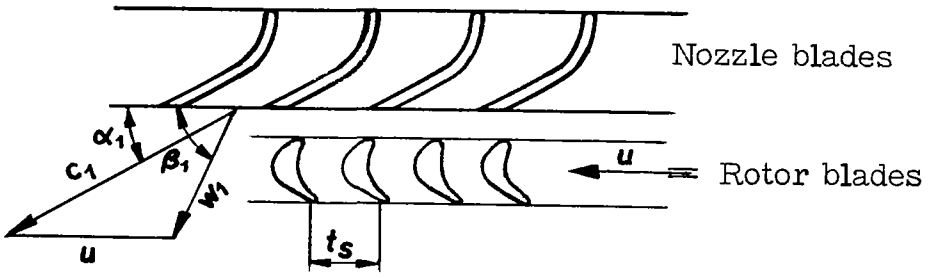

Figure 1.- Cross section through the blading.

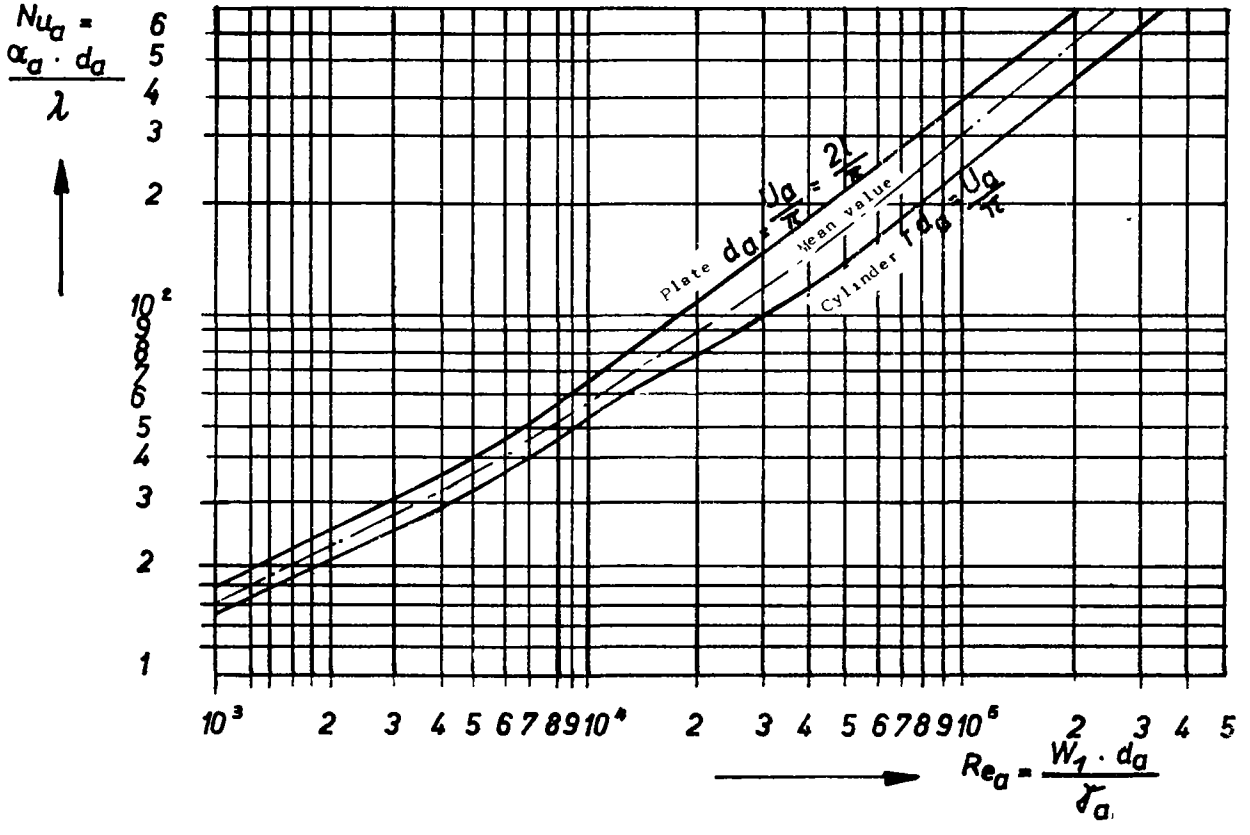

Figure 2.- Heat transfer at the blade profile.

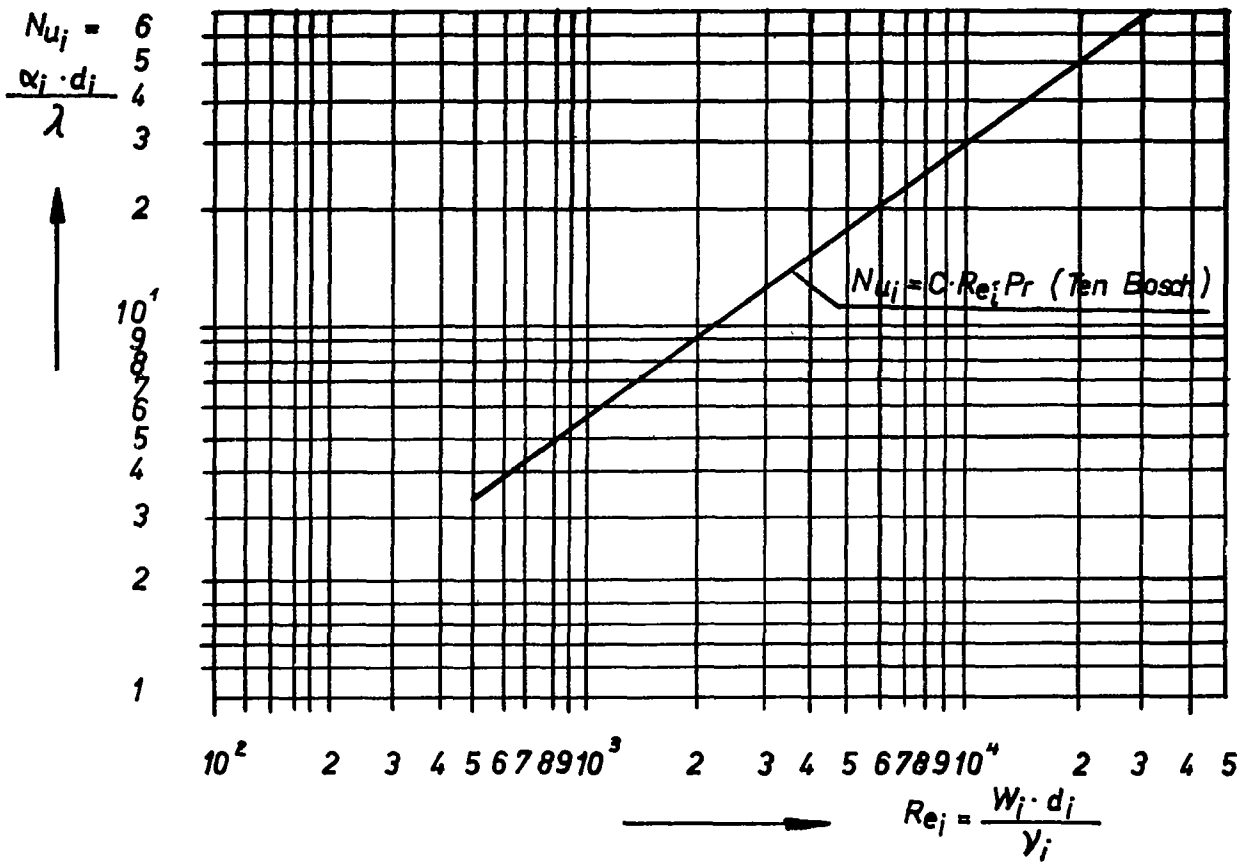

Figure 3.- Heat transfer in the cooling duct.

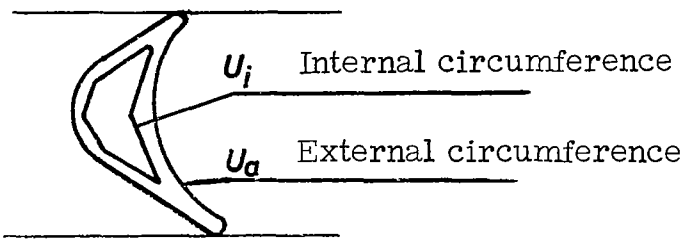

Figure 4.- Cross section through a hollow blade.

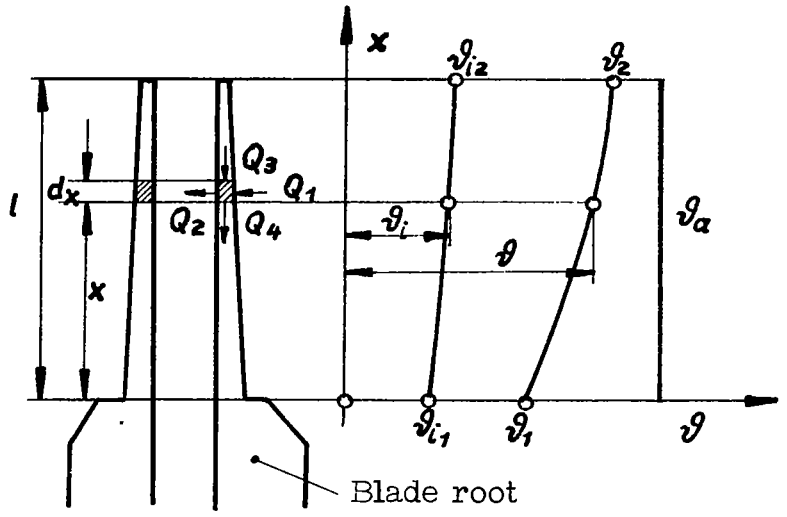

Figure 5.- Temperature variation at the blade.

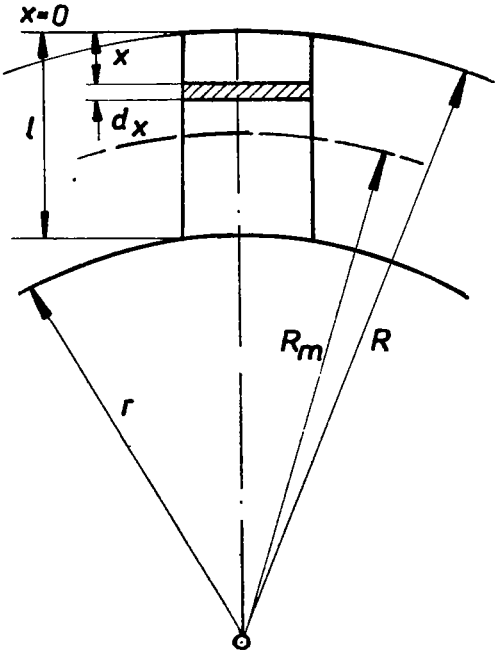

Figure 6.- Cylindric blade.

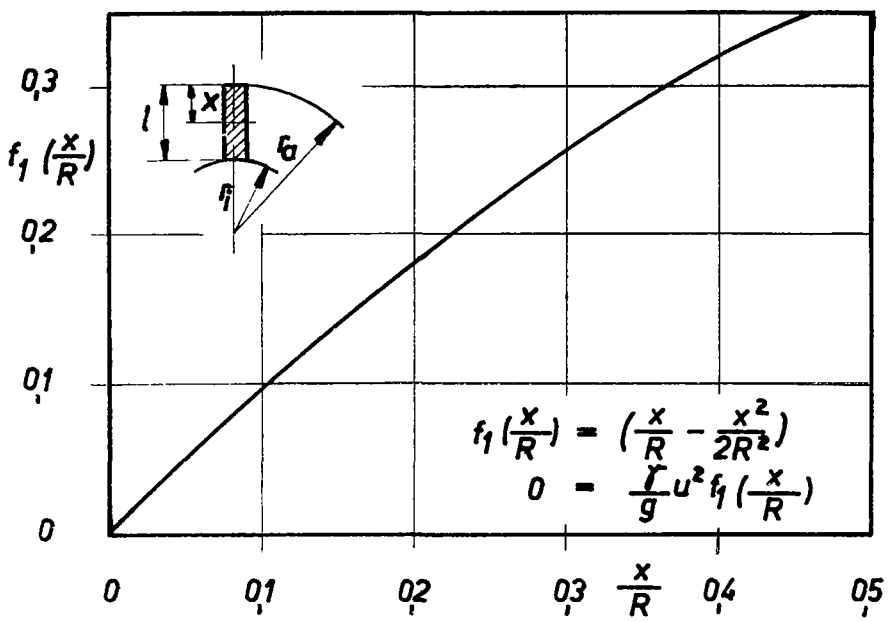

Figure 7.- Stress function for the cylindric blade.

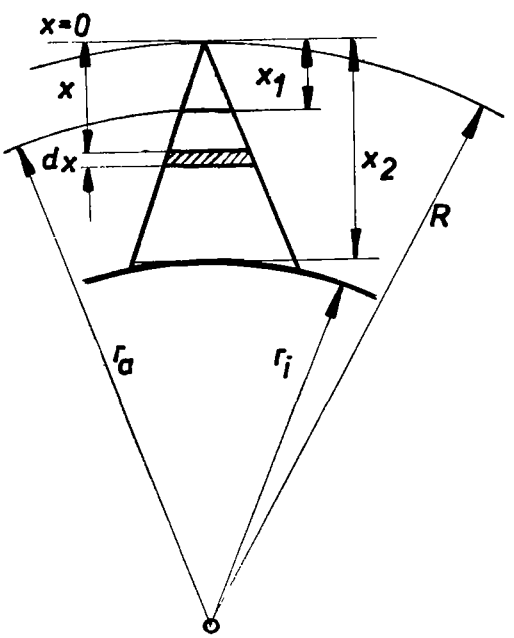

Figure 8.- Blade.

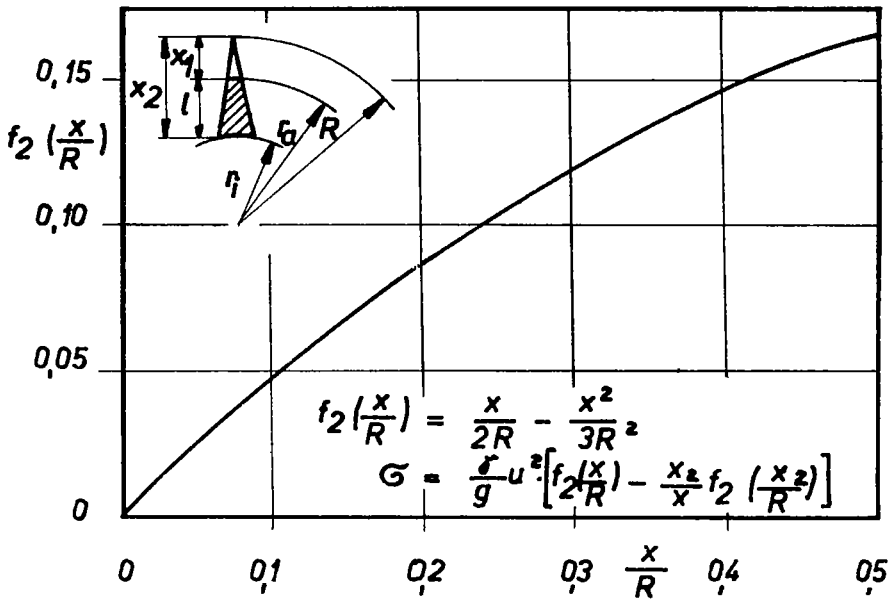

Figure 9.- Stress function for the tapered blade.

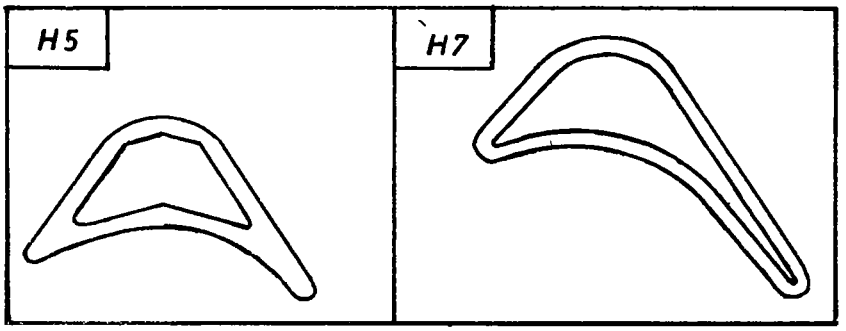

Figure 10.- Cross section of two hollow blades.

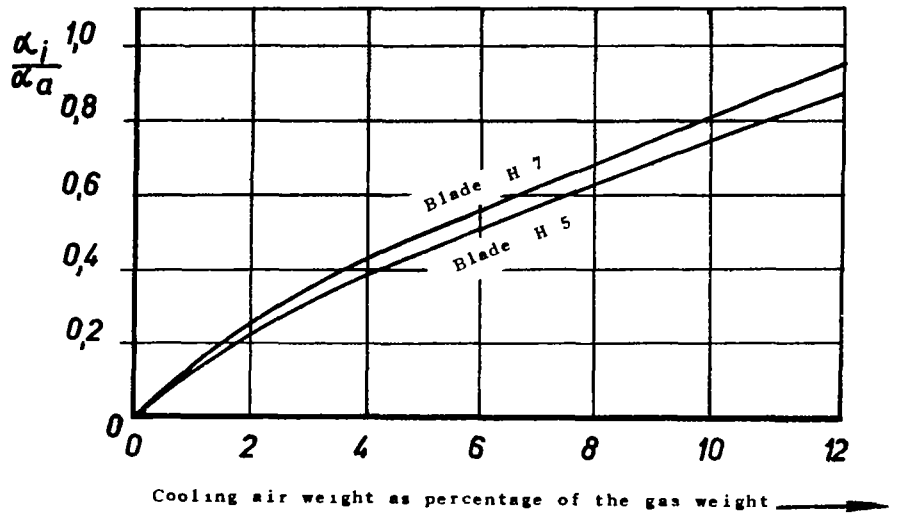

Figure 11.- Ratio of the heat transfer coefficients as a function of the cooling air mass.

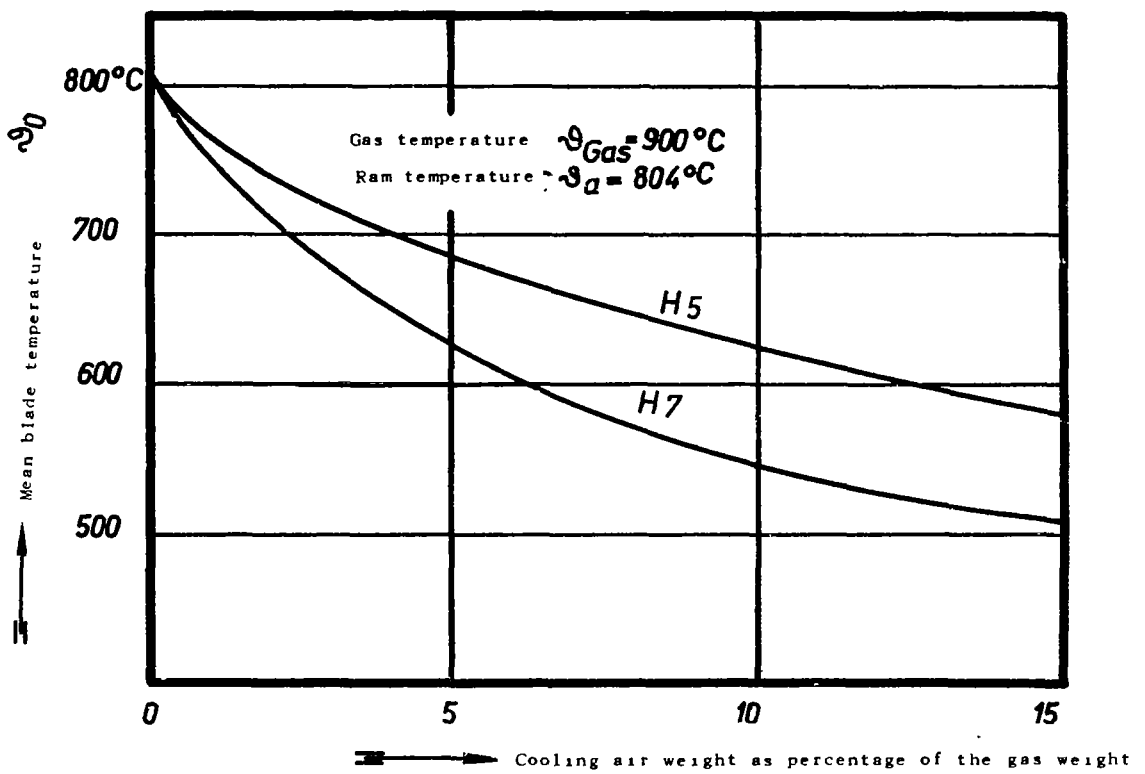

Figure 12.- Blade temperature as a function of the cooling air mass.

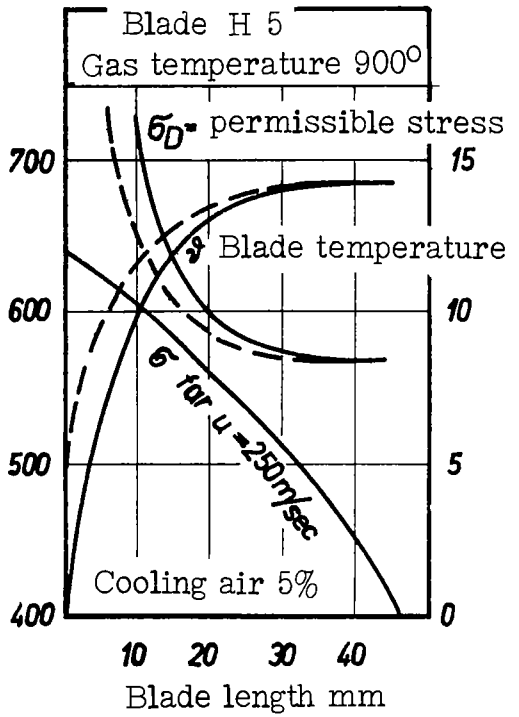

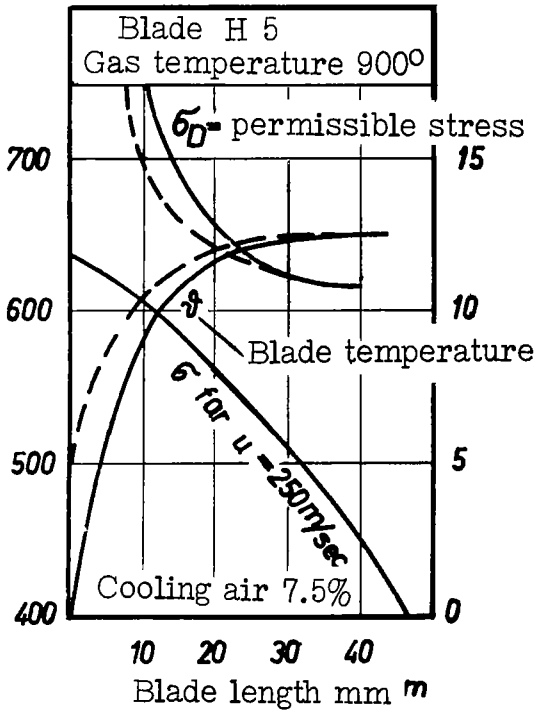

Figure 13.- Temperature variation and stress at the hollow blade H 5.

Figure 14.- Temperature variation and stress at the hollow blade H 5.

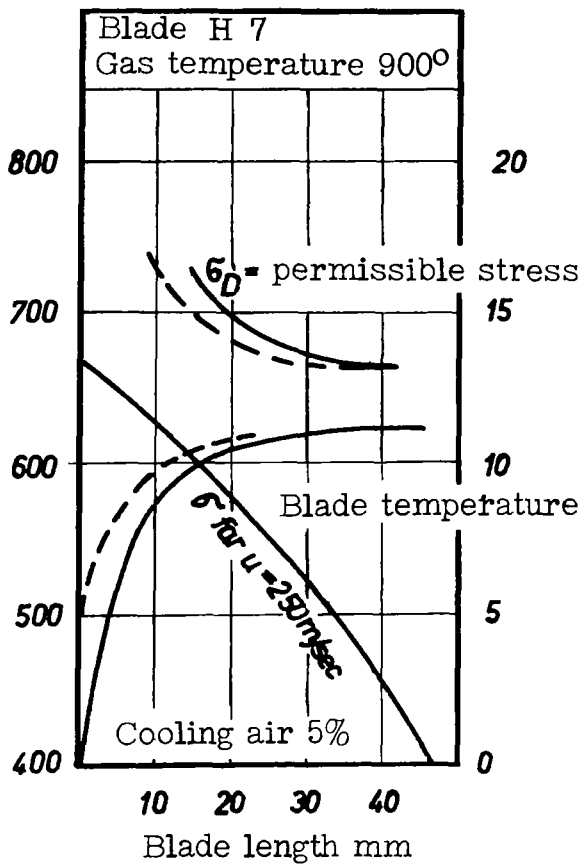

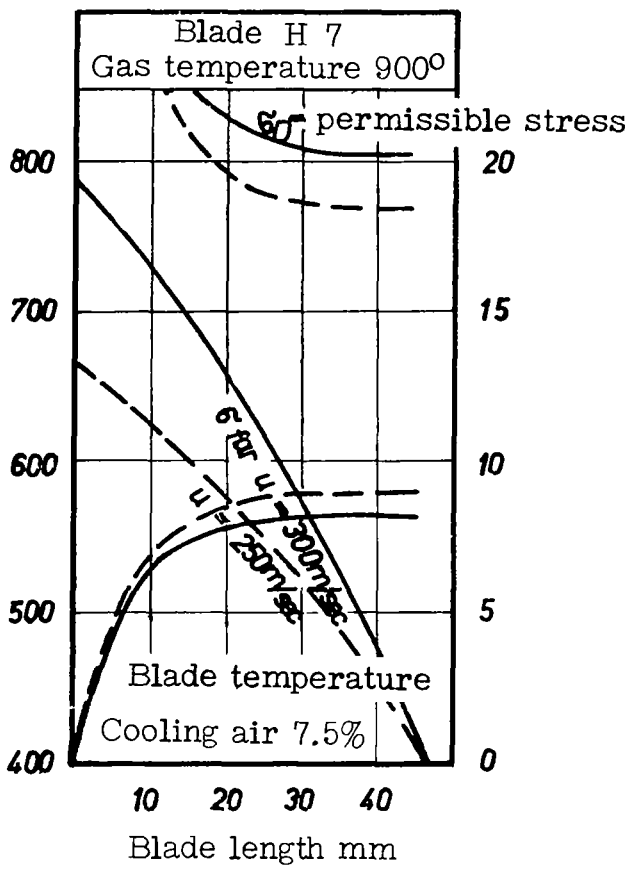

Figure 15.- Temperature variation and stress at the hollow blade H 7.

Figure 16.- Temperature variation and stress at the hollow blade H 7.

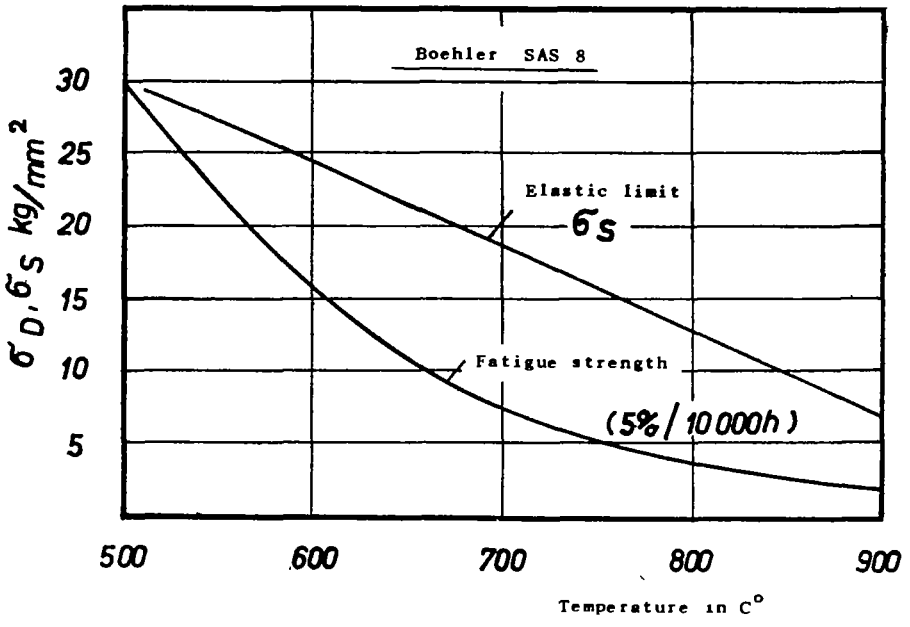

Figure 17.- Heat resistance of the material "SAS 8"

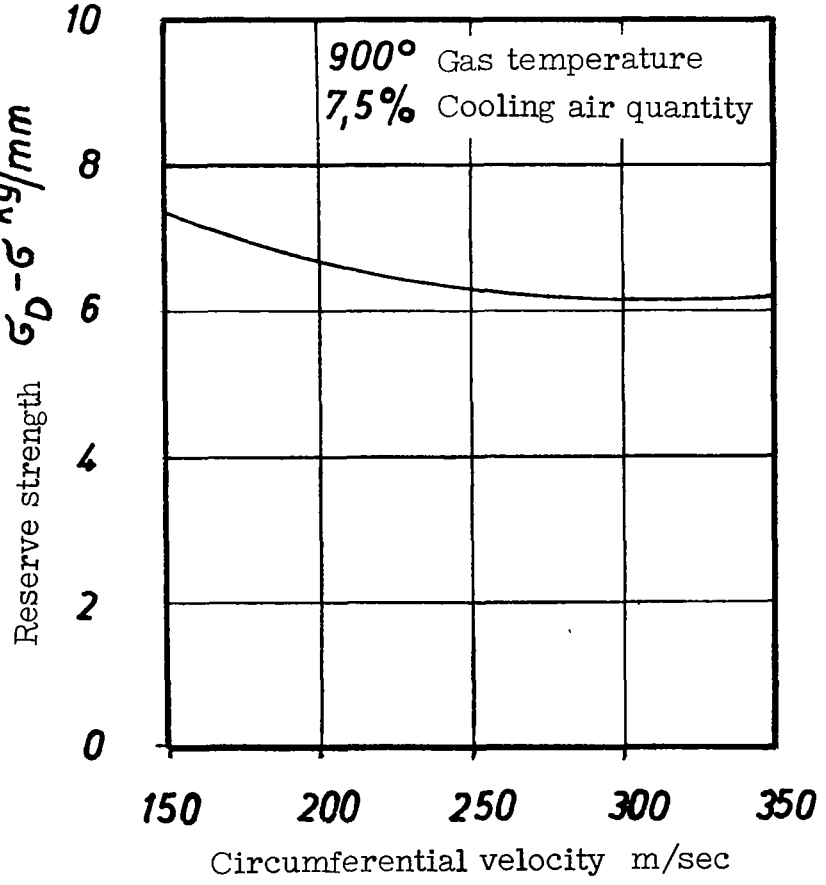

Figure 18.- Reserve strength as a function of the circumferential velocity.

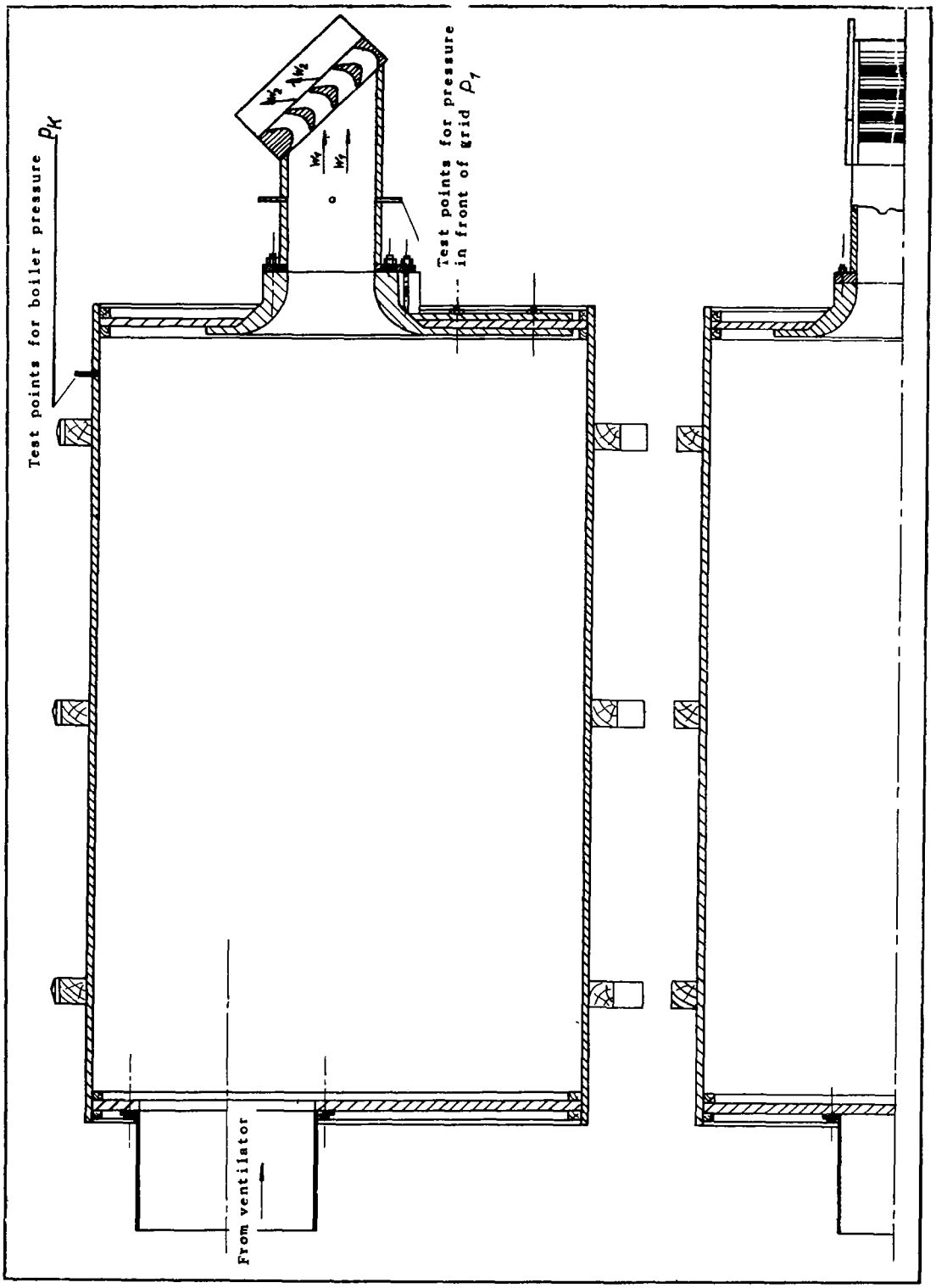

Figure 19.- Wind tunnel for cascade measurements.

Figure 20.- Blade cascade with nozzle.

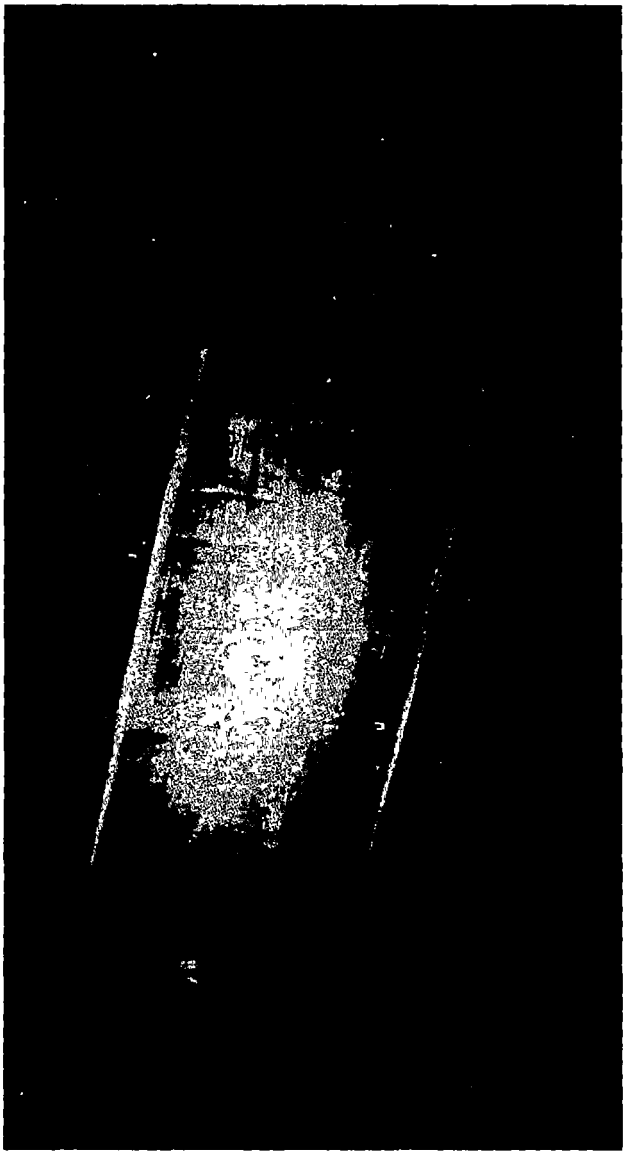

Figure 21.- Test blade.

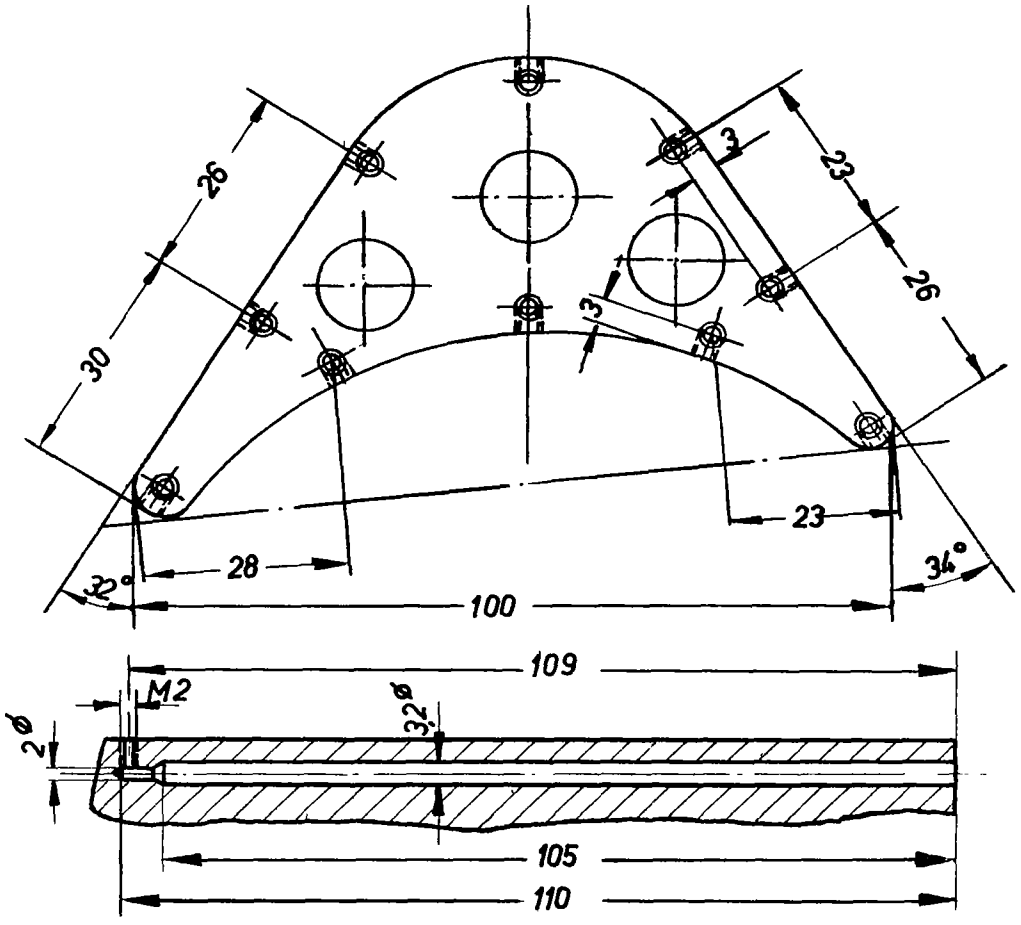

Figure 22.- Dimensions of the test blade.

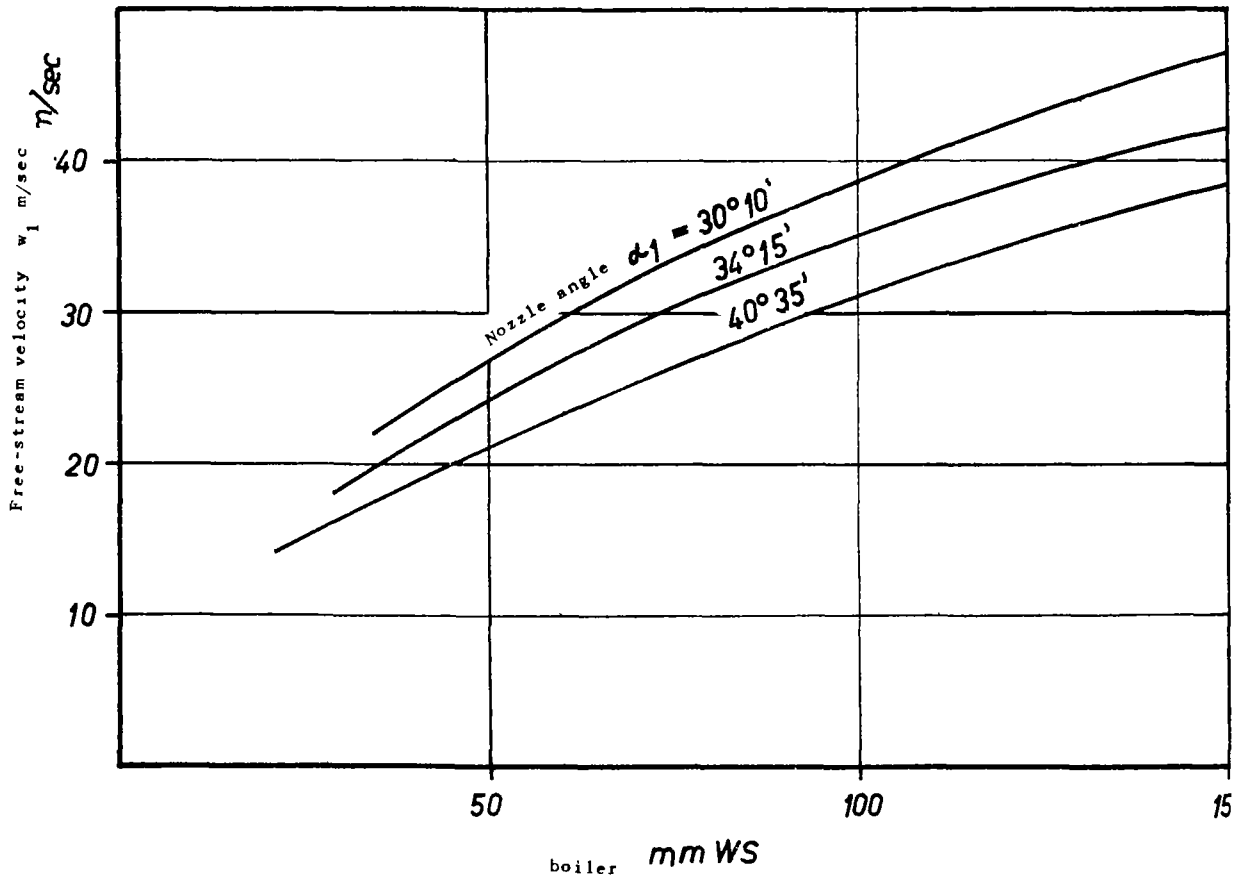

Figure 23.- Velocity as a function of the chamber pressure.

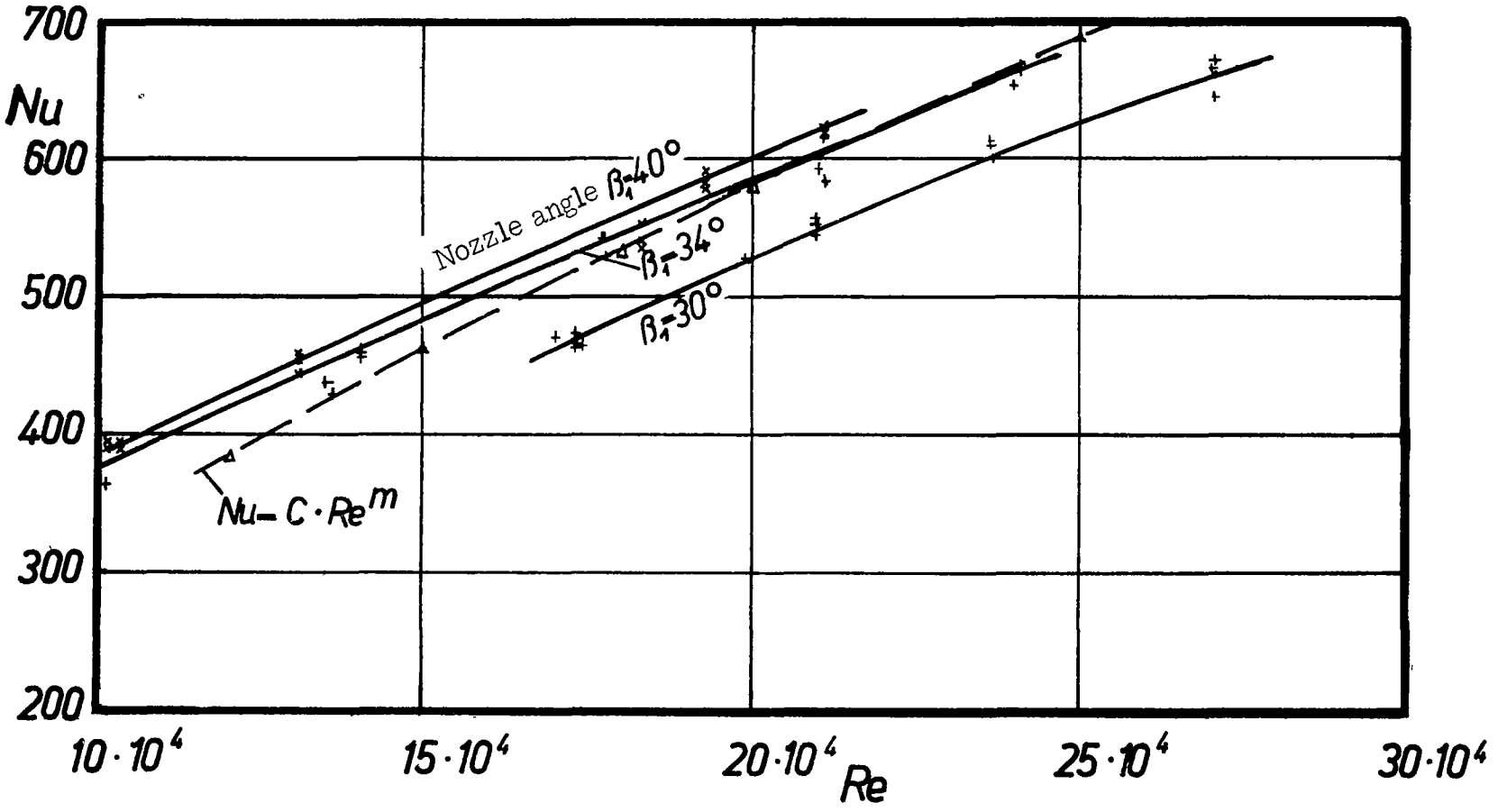

Figure 24.- Nusselt number for the blade profile H 3.

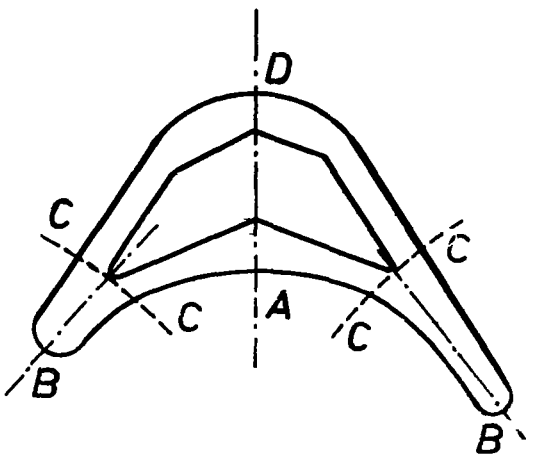

Figure 25.- Blade cross section.

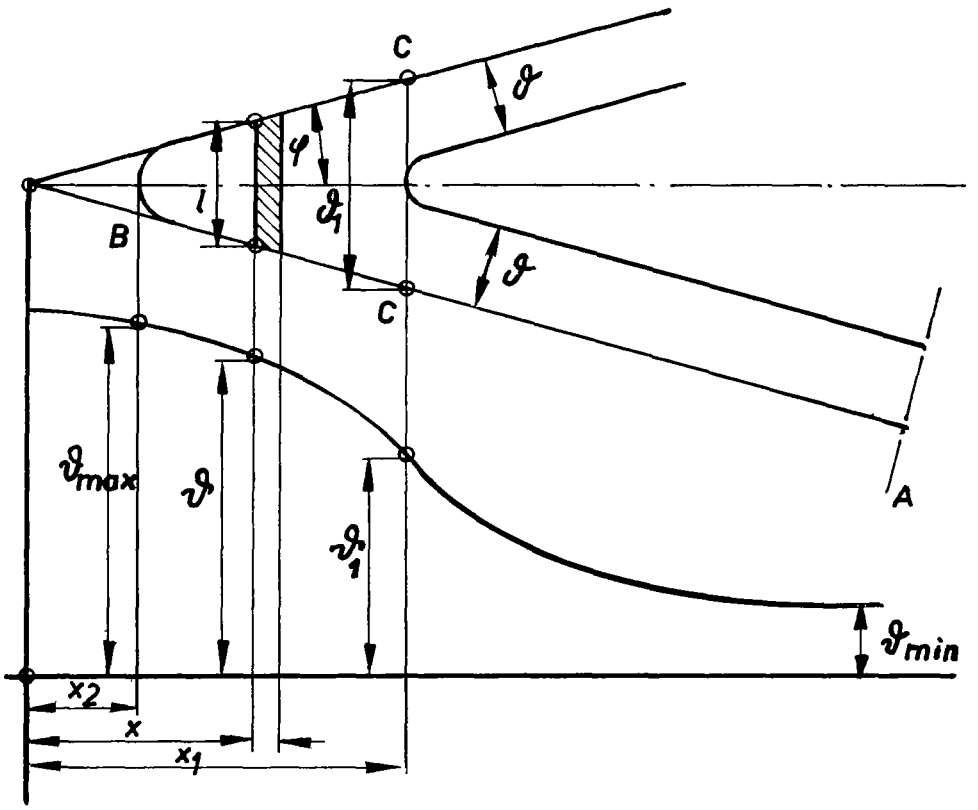

Figure 26.- Temperatures in the blade cross section.

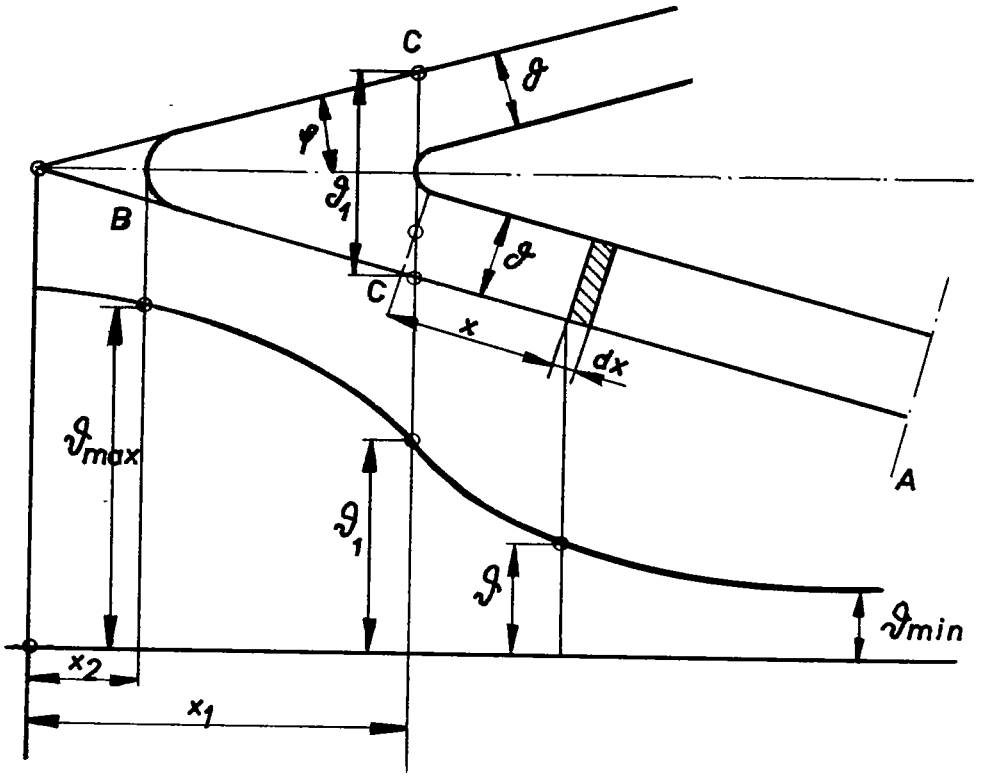

Figure 27.- Temperatures in the blade cross section.

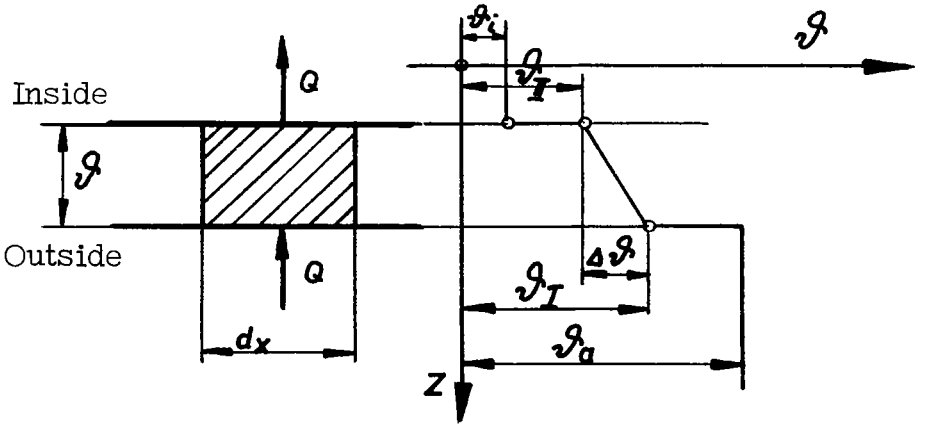

Figure 28.- Temperature drop in the blade wall.

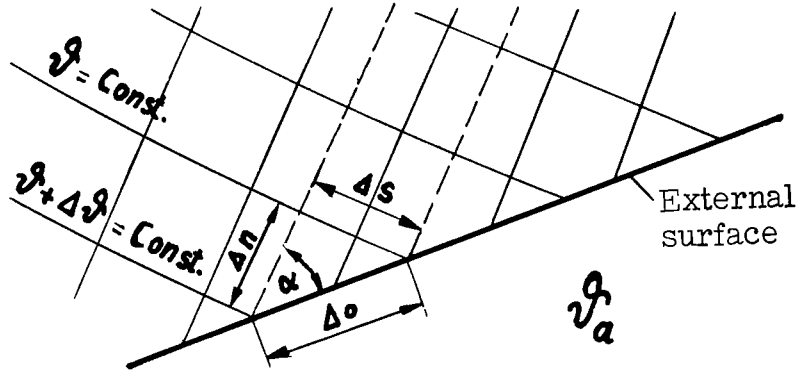

Figure 29.- Temperature field.

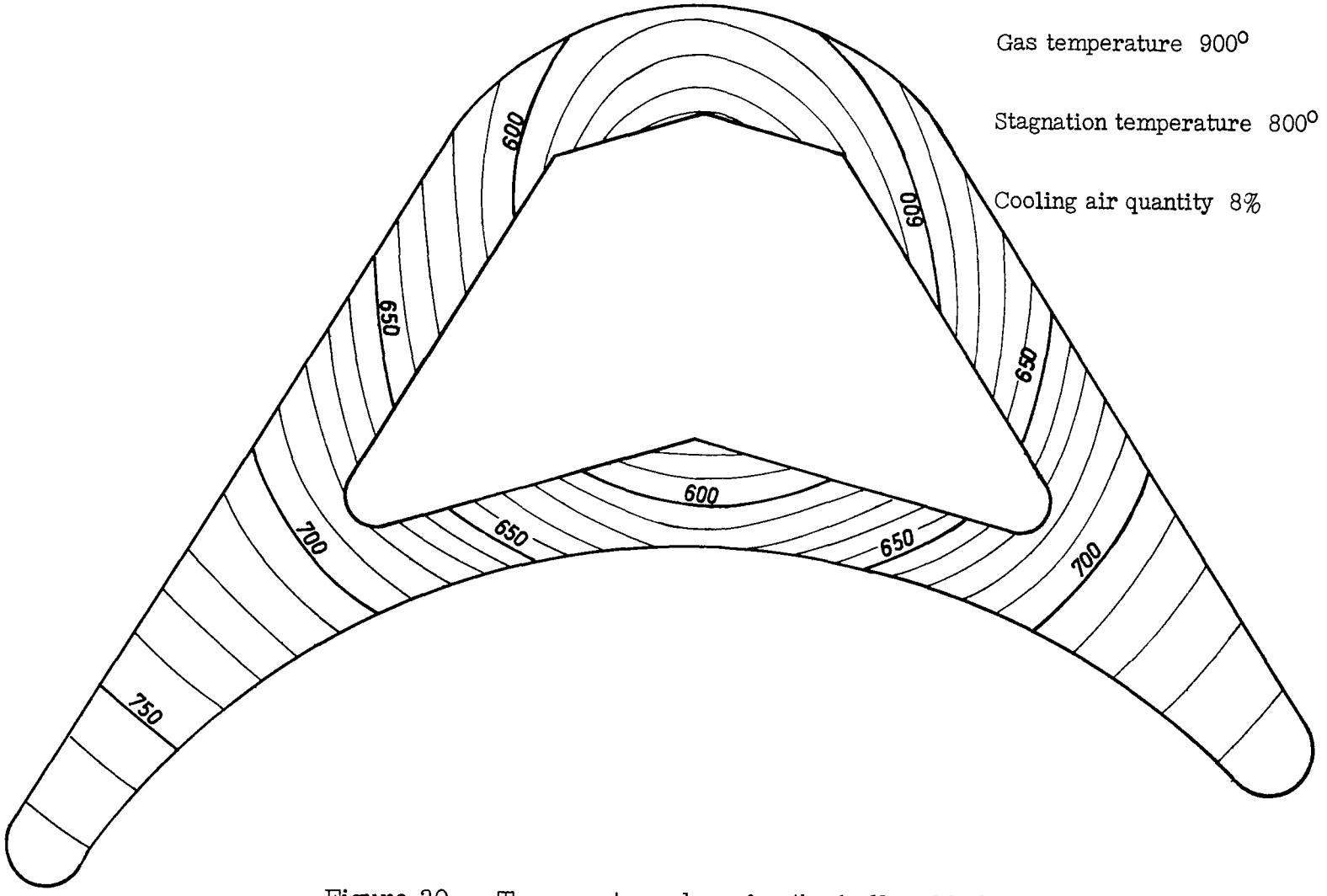

Figure 30.- Temperature drop for the hollow blade H 8.

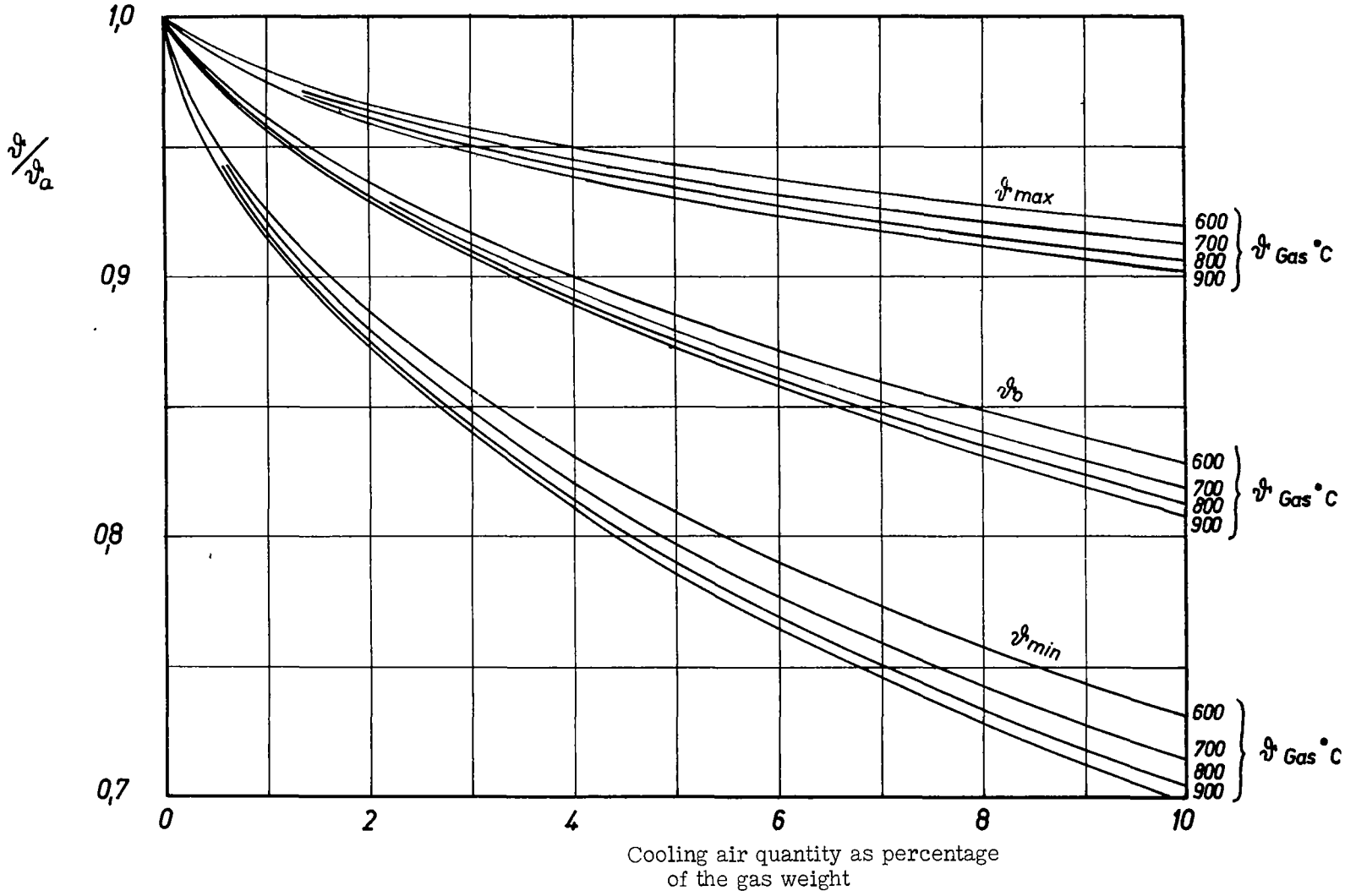

Figure 31.- Maximum, mean, and minimum temperature in the cross section of the blade H 5.

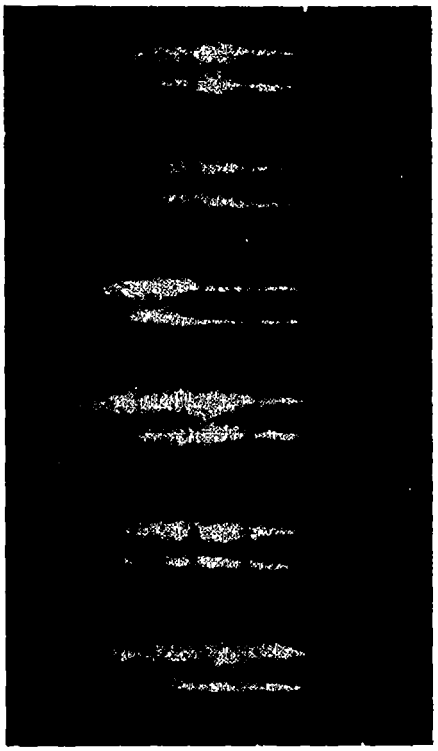

Figure 32.- Heat cracks on a blade.

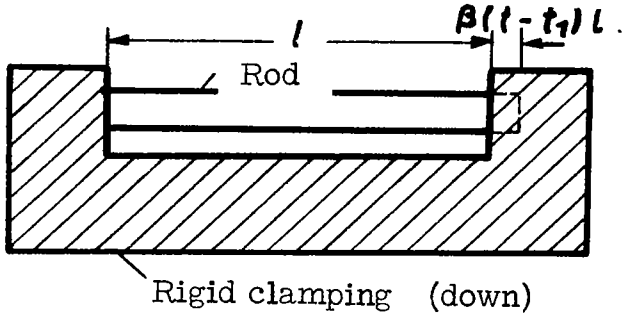

Figure 33.- Rod with rigid clamping.

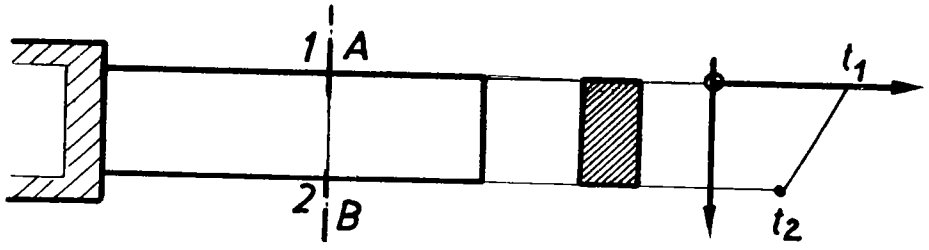

Figure 34.- Rod clamped on one end.

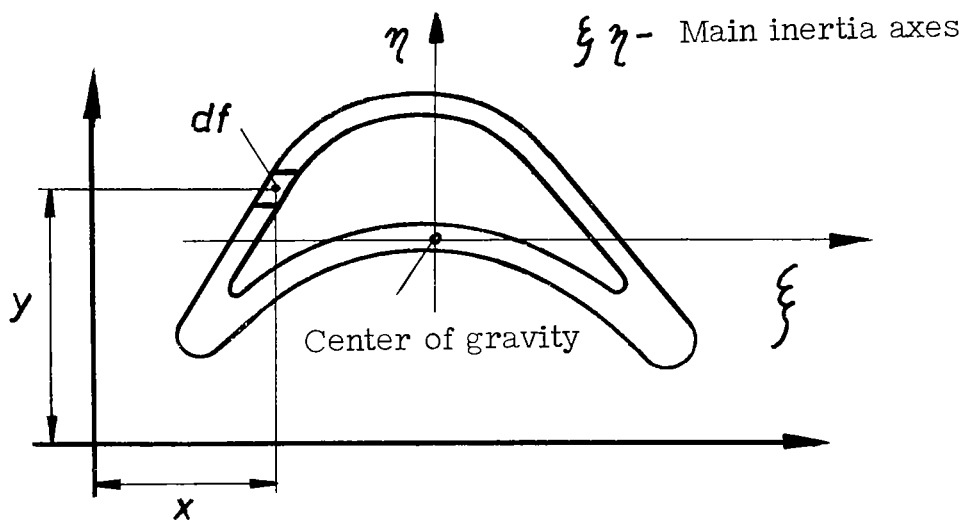

Figure 35.- Cross section of a hollow blade.

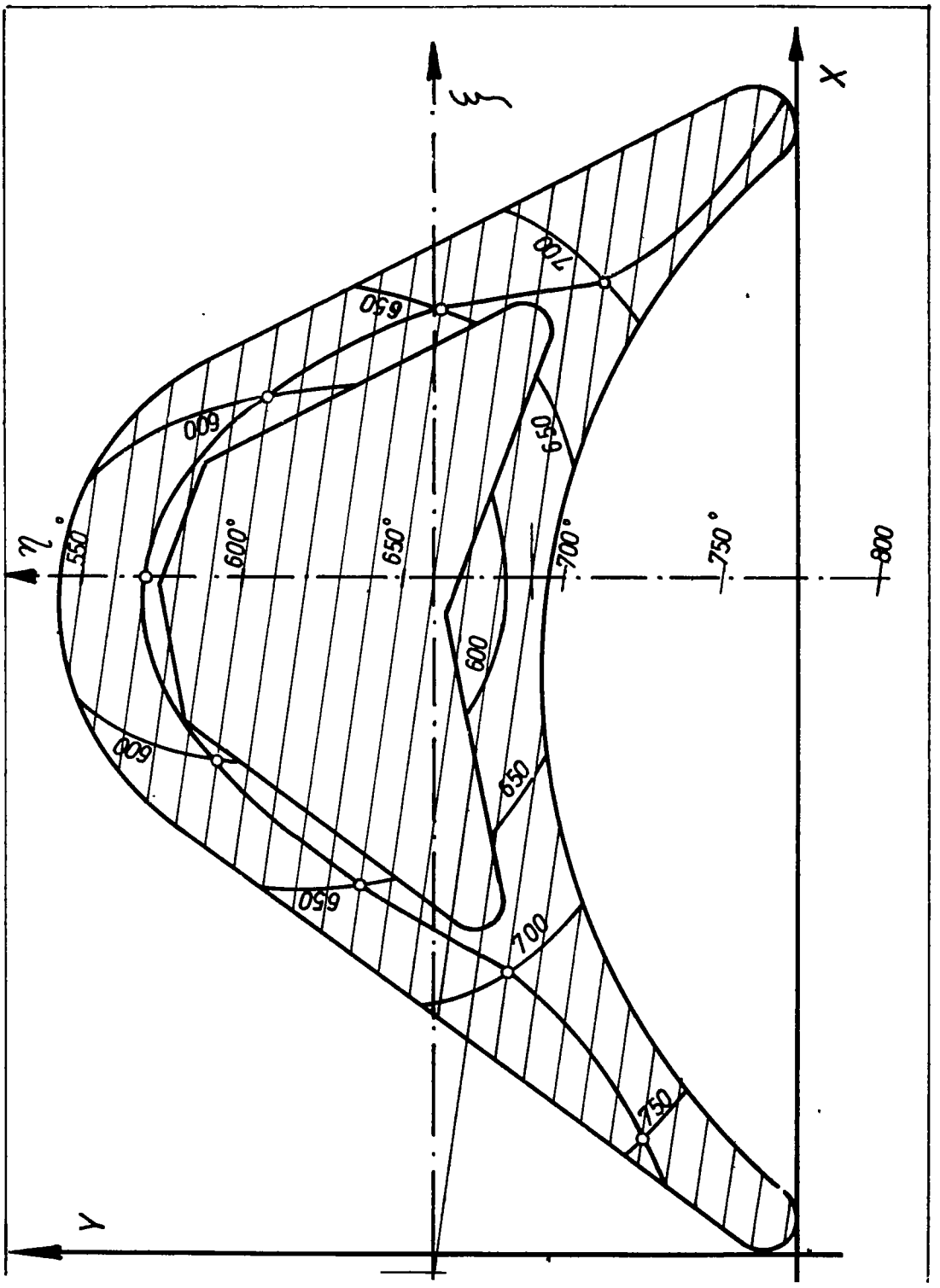

Figure 36.- Superposition of temperature field and temperature plane for the blade H 8.

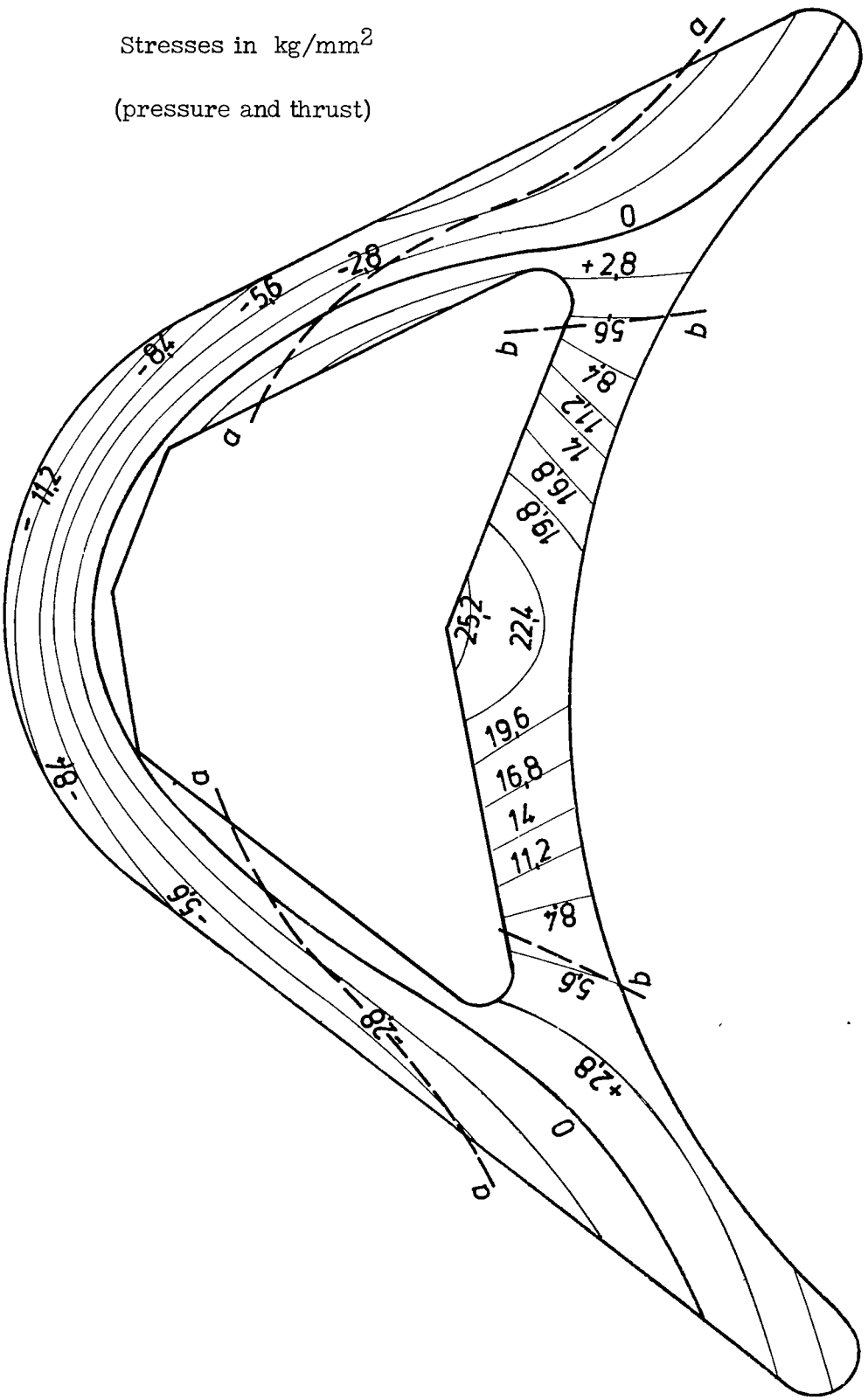

Figure 37.- Stress field for the hollow blade H 8.

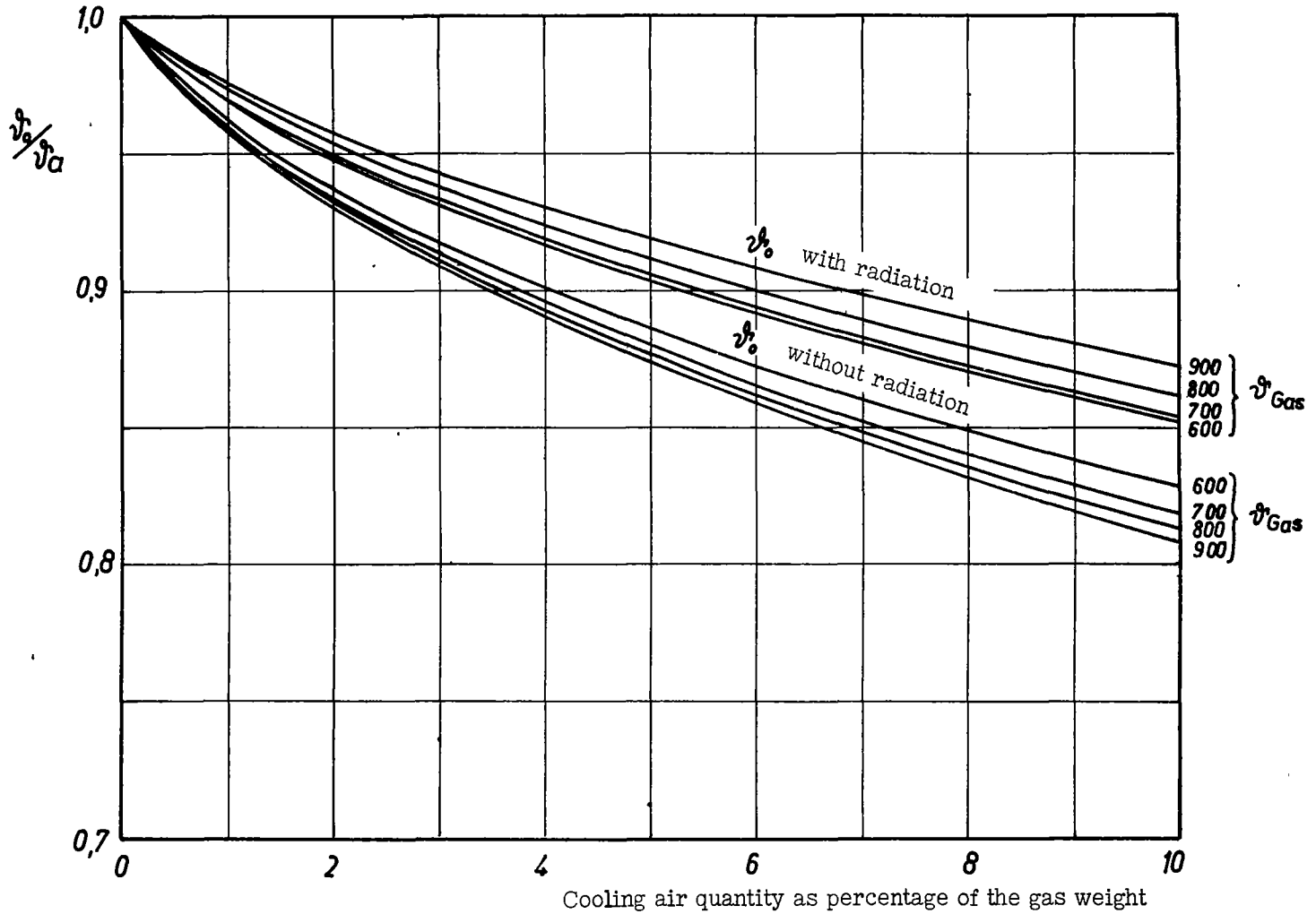

Figure 38.- Mean temperature of the blade H 3 with and without radiation.

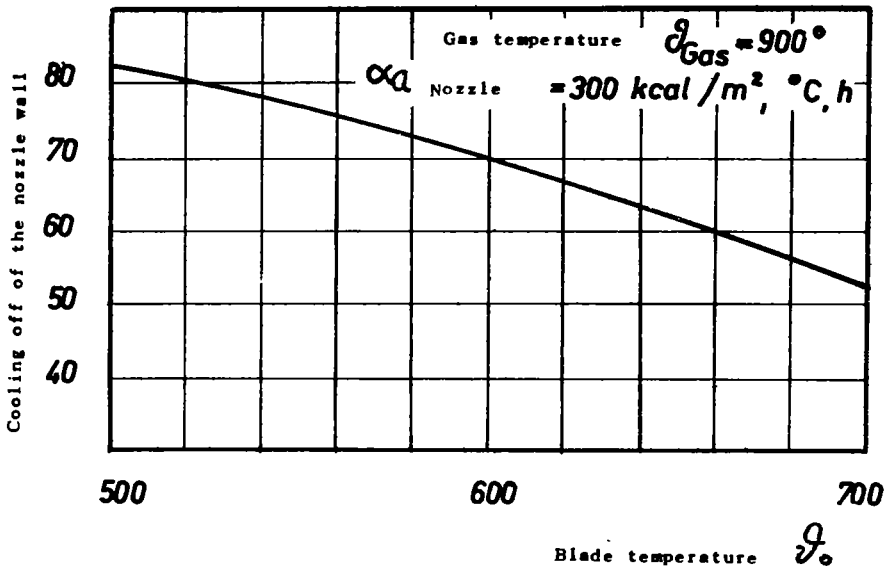

Figure 39.- Variation of the nozzle wall temperature by radiation.

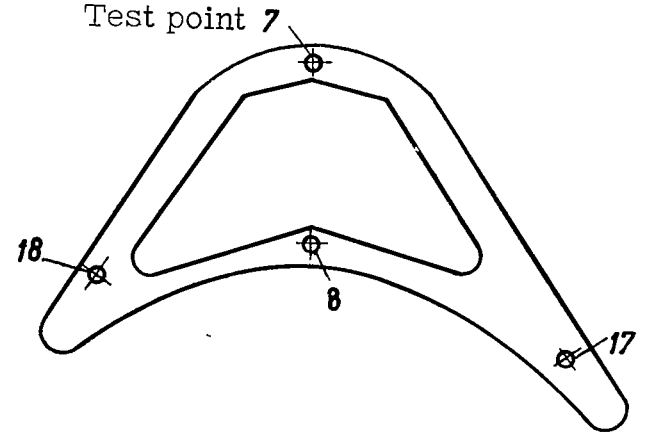

Figure 40.- Location of the test points in the blade cross section.

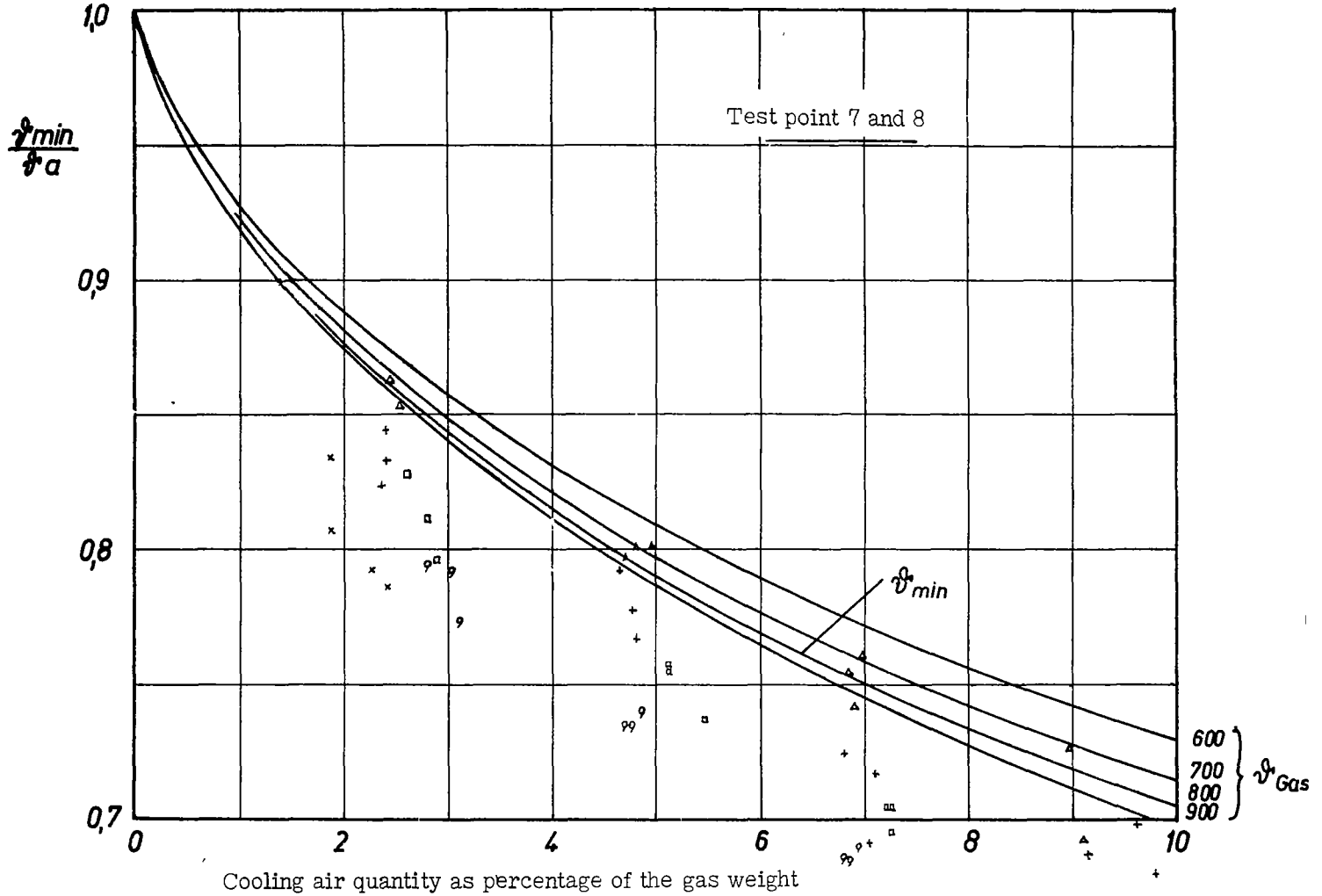

Figure 41.- Comparison of calculation and measurement for the minimum temperature in the blade cross section H 7.

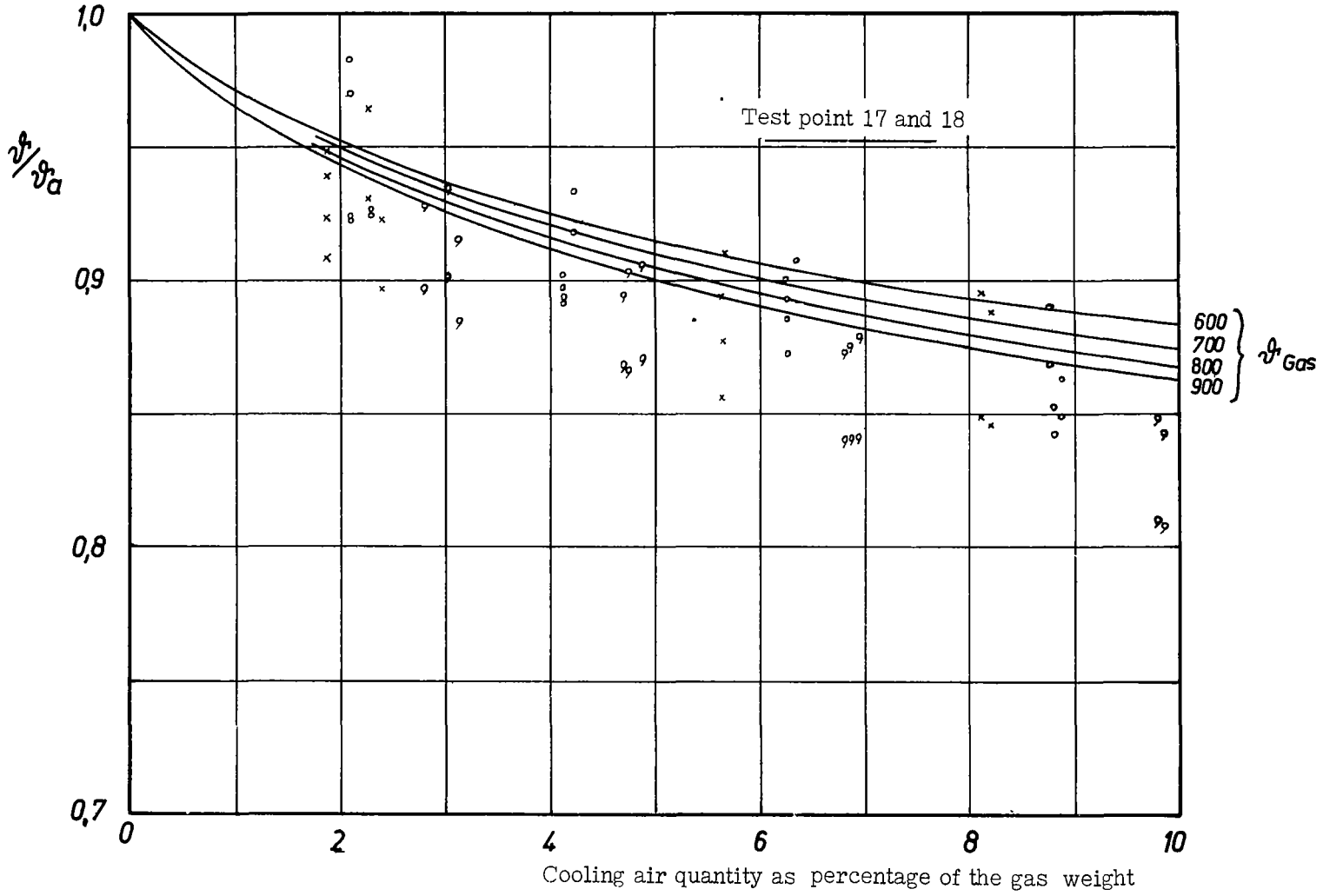

Figure 42.- Comparison of calculation measurement for the temperatures at the test points 17 and 18.

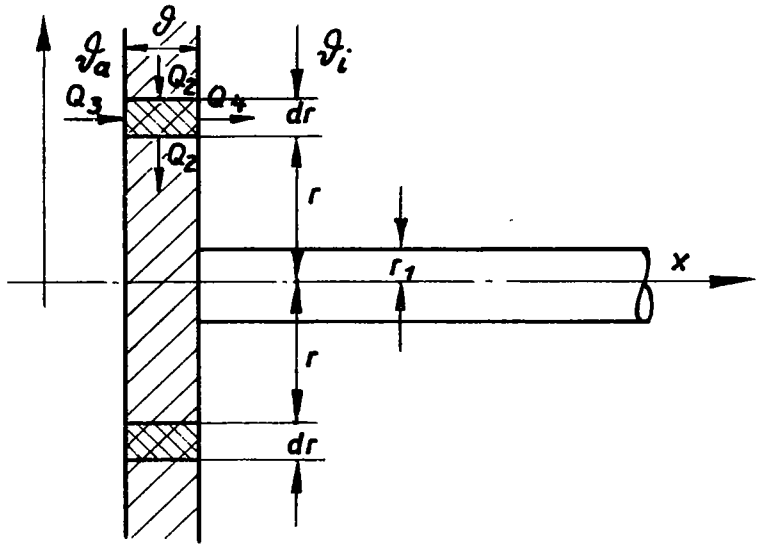

Figure 43.- Thermowire at the blade wall.

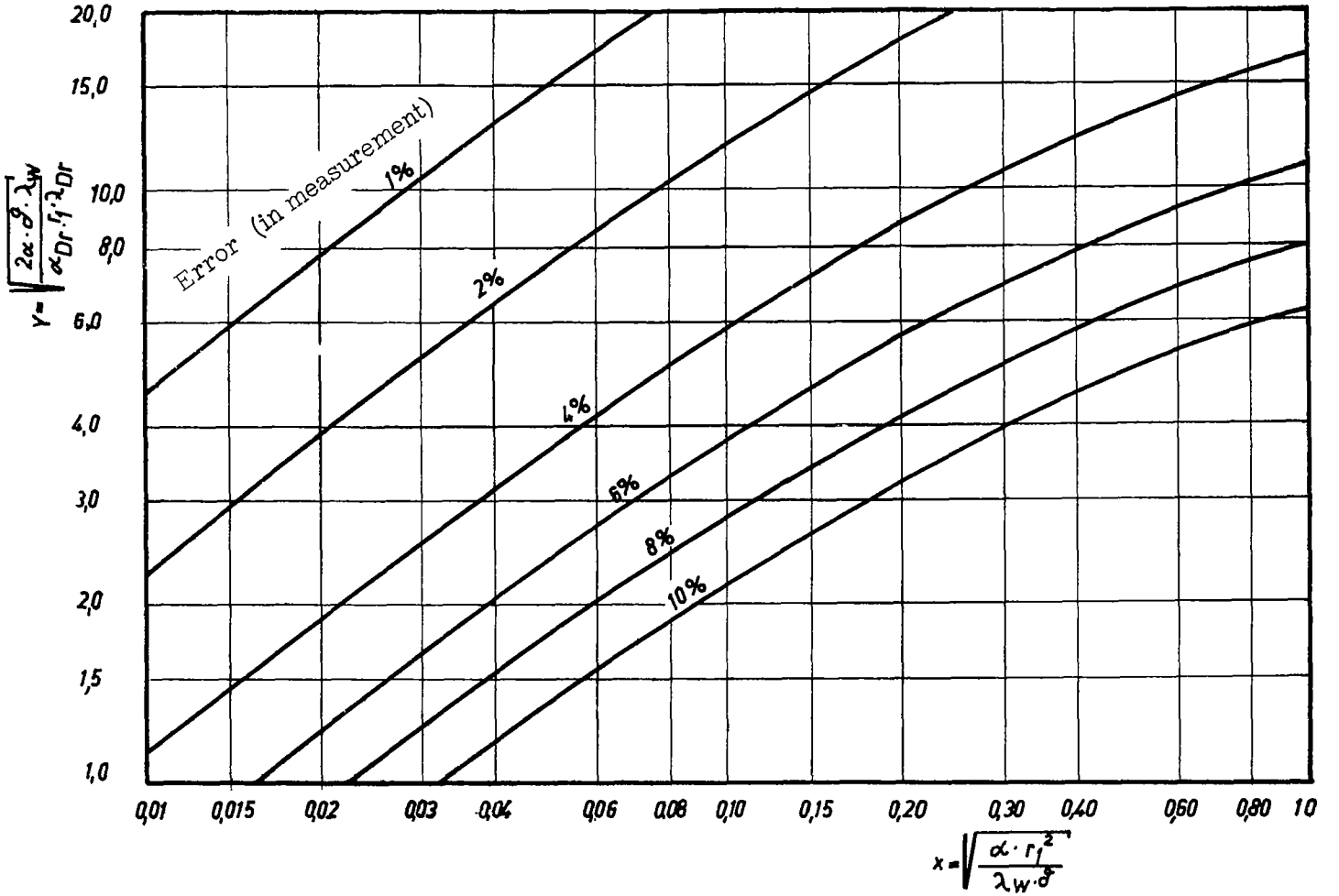

Figure 44.- Representation of the errors of measurement by thermowire.

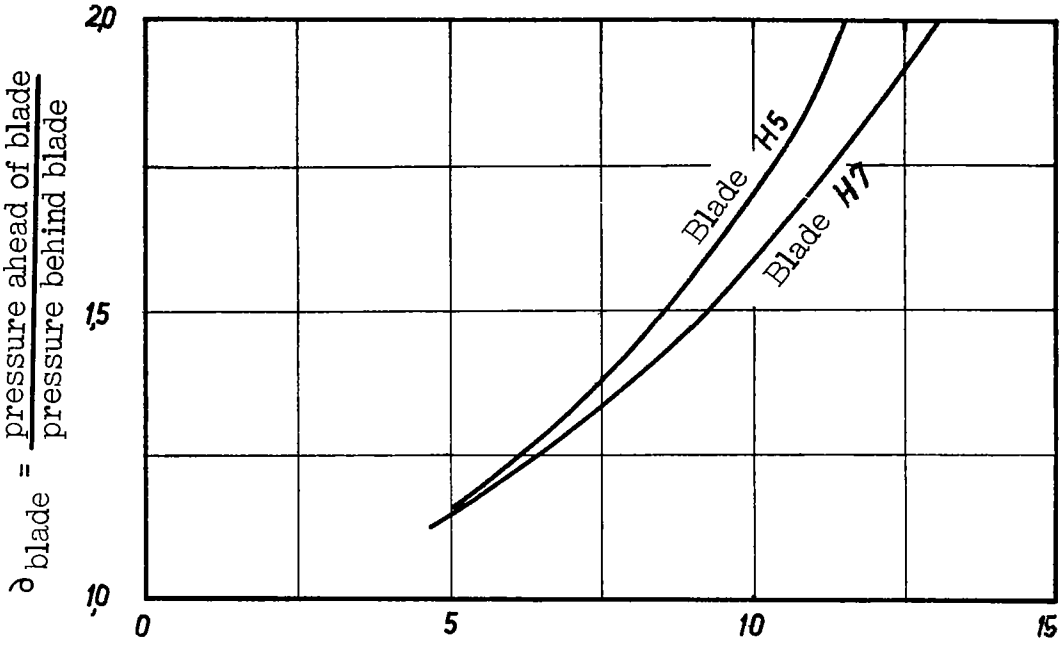

Figure 45.- Pressure ratio for the hollow blade.

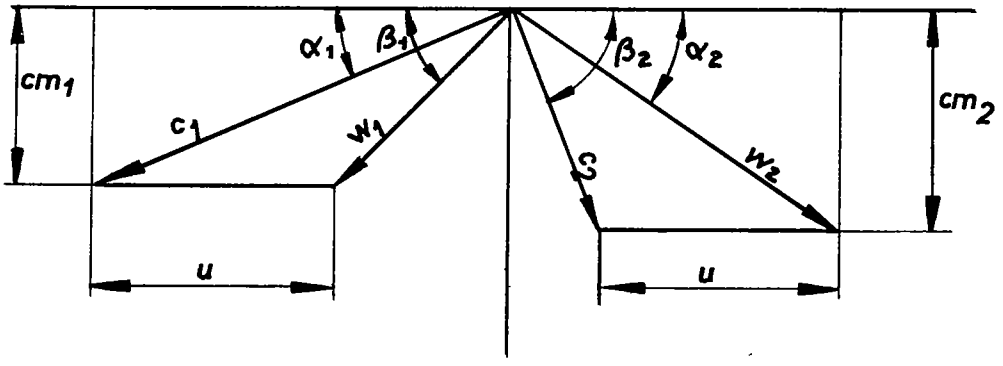

Figure 46.- Velocity triangle.

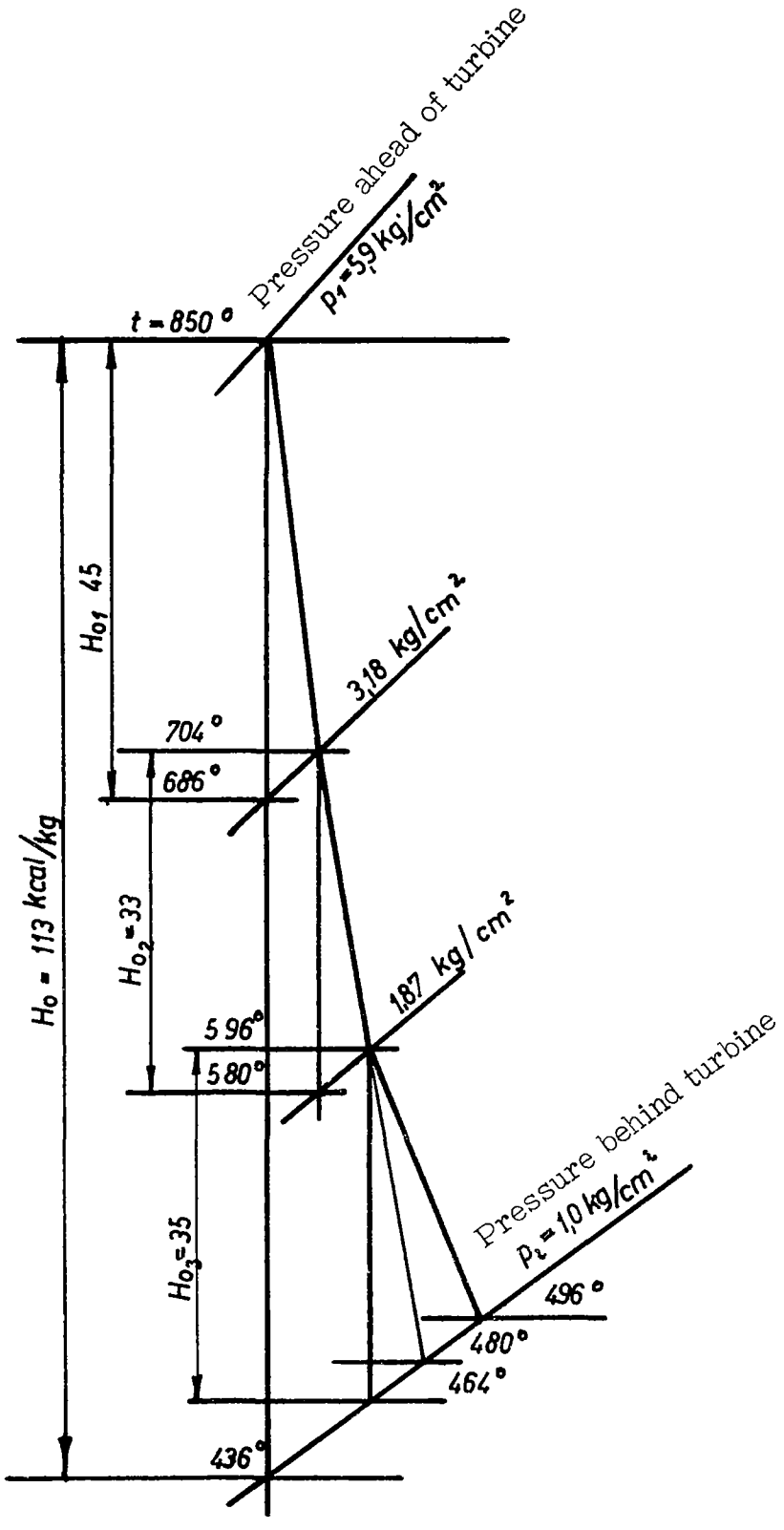

Figure 47.- J - S - diagram of a three-stage turbine apparatus.